Wood Fiber Polyamide Composites for Automotive Applications

by

Andrea Buchenauer

A thesis

presented to the University of Waterloo

in fulfillment of the

thesis requirement for the degree of

Master of Applied Science

in

Chemical Engineering

Waterloo, Ontario, Canada, 2016

Author's Declaration

I hereby declare that I am the sole author of this thesis. This is a true copy of the thesis, including any required final revisions, as accepted by my examiners.

I understand that my thesis may be made electronically available to the public.

Abstract

The automotive industry is currently experiencing environmental, legislative, and consumer pressure to improve the environmental sustainability of passenger vehicles. Just one of the approaches being taken to address this issue is the reconsideration of materials used in automotive application. The purpose of this thesis is to reduce the material weight and increase the environmental sustainability of polyamide composites in automotive parts. Specifically, an objective is to evaluate various types of polyamide and wood fiber blends and compare the mechanical and thermal properties with the intention of replacing glass fiber composite. The lower density of wood fibers could introduce weight savings that would improve fuel efficiency.

Two industrial sources of natural wood fiber are considered. These fibers are referred to as Suzano fiber and Woodforce fiber. The primary difference between these fibers is the type of processing. The polyamides compared include PA 6,10, PA 10,10 and recycled PA 6. Additionally, a hybrid blend of 30% PA 6,10 and 70% PA 6 is investigated. Composites are prepared through twin screw extruding and injection molding. The thermal and mechanical properties are measured through TGA, DSC, flexural tests, tensile tests, and Izod impact tests.

Due to the high melt temperature of polyamide, one of the main challenges of natural fibers is the thermal degradation that occurs. The use of ultraviolet light treatment is briefly investigated on the wood fibers in consideration, however it determined to be unnecessary for higher cellulose level fibers. In addition to comparing thermal behaviour of composites, alternative options addressing the issues associated with thermal degradation are explored through carbon fiber and odor adjusting additive.

Through thermal and mechanical comparisons, it was determined that the Suzano fiber had the highest improvement of mechanical properties when compounded with each polyamide. However, the disadvantage of the Suzano fiber is its ability to feed into the

processing equipment. By replacing the Suzano fiber with cellulose, it was determined that overall, the 20% cellulose level resulted in the most favourable combination of properties.

The blending of RPA 6 and PA 6,10 generally resulted in intermediate property values however did not offer any significant advantages. The use of PA 6,10 is good for sustainability because of its bio-content but must be balanced with the additional cost.

Acknowledgements

I'd like to express the deepest gratitude to my supervisor, Leonardo Simon, for all the support, guidance, and encouragement. Thank you so much for this opportunity.

Special thanks to Ford Motor Company for funding my academic program and for providing use of their research facilities.

I'd also like to thank the Ford Research and Innovation Team for all the help and training provided. Specifically, thanks to Alper Kiziltas for the direction with experimental planning. Many thanks to Ron Koslakiewicz, James Burkholder, and John Rizzo for the experimental assistance.

Finally, I'd like to thank Professor Michael Pope and Professor Aiping Yu for generously giving their time to be part of my thesis Reading Committee.

Table of Contents

List of Figures

List of Tables

1.0 Introduction

1.1 Motivation and Objectives

Motivation

Since 1975, the national highway traffic safety administration (NHTSA), in the United States, has held a corporate average fuel economy (CAFE) standard that requires vehicle manufacturers to meet a minimum level of fuel economy across their assortment of vehicles. From 1990 to 2010, the fuel economy for passenger cars was held at 27.5 miles per gallon [1]. In 2010, a presidential memorandum was issued requesting strong action be taken to address climate change and reduce oil consumption [2]. In response, the CAFE standards were increased to be more demanding. Although already improved, goals for the 2017-2025 national program continue to challenge vehicle manufacturers. By 2017, the estimated fleet-average requirement is expected to be around 35.1 mpg [2]. Agencies predict that in order to meet these standards, the estimated cost of a vehicle will increase by $1,800 USD. However, the improved fuel economy would save the consumer $3,400-$5,000 over the lifetime of the vehicle [2]. From the manufacturing perspective, cost savings, while still implementing new technologies is desired.

This heightened requirement for fuel economy has greatly sparked interest in light-weighting. This concept originates fundamentally from Newton's second law through the understanding that it takes less energy to accelerate a lighter object. It is estimated that a 10% reduction in vehicle weight can improve the fuel economy by 6-8% [3]. Although the majority of weight savings is focused on the heavier metal components, there is still opportunity for improvement in polymer materials. In many non-structural parts of the vehicle, polymer materials can replace metals without compromising on function while delivering weight reduction. Moreover, hybrid assemblies integrating multi-material

component (metal, fiber, polymers…) have opened up new opportunities for integration of function and light-weighting.

Polyamide is a polymer widely used in the automotive industry due to its processability and high thermal and chemical resistance [4]. In 2014, approximately 37 pounds of polyamide was used in a standard light vehicle [5]. Generally, polyamide is reinforced with short glass fiber in order to increase its modulus, strength and heat deflection temperature [4]. If the reinforcement of polyamide could be replaced with natural fiber, instead of glass fiber, the overall weight of the composite would be less due to the density of wood fiber being significantly lower than glass fiber [6].

In addition to fuel economy motivations, a holistic approach is needed for the design of automotive components. The highest priority factors will always include cost and quality. Components that are crucial to the operation and safety of a vehicle must meet meticulous standards. In consideration of the life cycle, fuel economy is just one factor. The source of materials and the method in which they are produced, as well as what happens to the parts at the end of use all contribute to the total carbon footprint associated with a single vehicle.

Objective

The purpose of this research is to explore the use of natural wood fibers as a filler in polyamide composites. Ford Motor Company sponsored a *Northern Star* research project at the University of Waterloo, the title of the project was "Lightweight Sustainable Thermoplastic Composites." The research work presented here was part of such initiative.

Because polyamide has a high melting temperature, it is ideal for use in relatively high temperature applications, such as near a vehicle engine. However, this same feature causes an issue with natural fiber filler because of thermal degradation. The use of natural fiber as a filler is sought after due to its environmental benefits as compared to traditional fillers, such as fiberglass. However, the effects of thermal degradation can jeopardize the

structural integrity of a component. The ambition of this project is to find a solution that increases the sustainability and environmental friendliness of a polyamide composite for use in automotive applications. Through investigation of specific commercially available products, the objective is to find a suitable combination of polyamide and natural fiber such that it is stable at process temperatures and at the lowest cost.

1.2 Scope

Initially, two sources of natural wood fiber are considered. The first fiber is a eucalyptus pulp that is produced by Suzano Group, referred to hereafter as Suzano fiber. The second source of fiber, referred to as Woodforce fiber, is manufactured by Sonae Industria. Woodforce fiber is an engineered diced pellet designed for use as a polymer reinforcement. Woodforce provided two types of fiber samples, subsequently labelled Woodforce 1 and Woodforce 2.

Three types of polyamide are considered. These included PA 6,10, PA 10,10, and recycled PA 6. In addition, the option of combining polyamides to create a hybrid product is explored.

Beyond the investigation of fiber and polyamide types, two alternative solutions are addressed in the interest of rectifying the effects of thermal degradation occurring. First, the use of carbon fiber in addition to natural fiber is performed to recuperate lost properties. In addition, an additive that hides the smell of thermal degradation is used and effects on mechanical properties are analysed.

The thermal properties of the fibers in consideration are compared prior to compounding. Once compounded, the mechanical properties evaluated include flexural properties, tensile properties, and notched Izod impact strength. Some other areas that would be relevant to this application, but are not included in the scope of this thesis, include rheological properties, moisture absorption, and use of process additives.

1.3 Thesis Layout

This thesis is composed of 8 sections, the layout of which is summarized in Table 1. In the first section, the project is introduced and outlined. The second section provides the relevant background and previous research associated with the project. Section 3 outlines the experimental procedures that were applied to get the results. These results are organized and discussed in sections 4, 5, and 6. Finally, conclusions are provided in section 7 with some follow up recommendations given in section 8.

Table 1: Thesis Layout

1.0 Introduction			
2.0 Literature Review			
3.0 Experimental			
4.0 Thermal Stability of Wood Fibers			
Materials		Processing	Characterization
Suzano Fiber Woodforce 1 Woodforce 2		*Ground, Dried, UV treatment*	*TGA*
5.0 Initial Fiber and Polyamide Compounding			
Materials		Processing	Characterization
Suzano Fiber Woodforce 1 Woodforce 2	*RPA 6 PA 610 PA 1010*	*Extrusion Injection Molding*	*Flexural Tests Impact Tests*
6.0 Cellulose Compounding with a Polyamide Blend			
Materials		Processing	Characterization
Cellulose Carbon Fiber RP17	*RPA 6 PA 610*	*Extrusion Injection Molding*	*Flexural Tests Tensile Tests Impact Tests TGA, DSC, SEM*
7.0 Conclusions			
8.0 Recommendations			

2.0 Literature Review

2.1 Polyamide

2.1.1 Types of Polyamide

A polyamide is defined as any high molecular weight polymer that has amide linkages along the backbone structure [7]. Polyamides are semi-crystalline polymers, which mean they have some amount of crystalline structure and some amount of amorphous chains [8]. Natural polyamides exist and are found in casein, soybean, and peanut proteins [7]. However, the much broader use of the term polyamide tends to refer specifically to the linear linkages, first synthesized by DuPont, who coined the name 'Nylon' to market their product under. The term nylon is used in this document as a common name for polyamides.

There are two main categories of polyamides, which are determined by the number of monomers used in polymerization [9]. The first group uses only one monomer in the polymerization process. Consequently, this monomer has an amine group on one end and a carboxyl group on the other. In between these two end groups is a chain of carbons. The number of carbons in the monomer chain determines the resulting name of the polymer. Figure 1 shows the monomer and resulting polymer chain for this type of nylon.
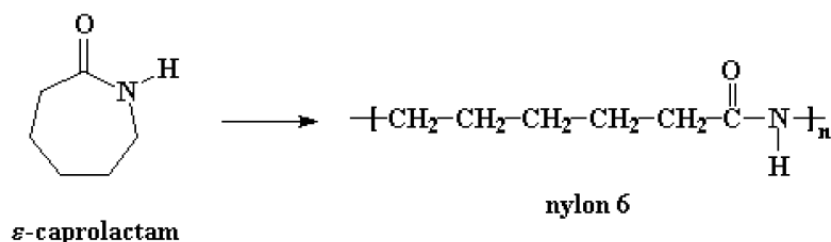
Figure 1 - Example of PA from Single Monomer [10]

The second group of polyamides requires two base monomer units in order to polymerize. One monomer has double amine end groups with a carbon chain separating the amines, while the other monomer is the same but with two carboxyl end groups. Figure 2 shows an example of this type of nylon.
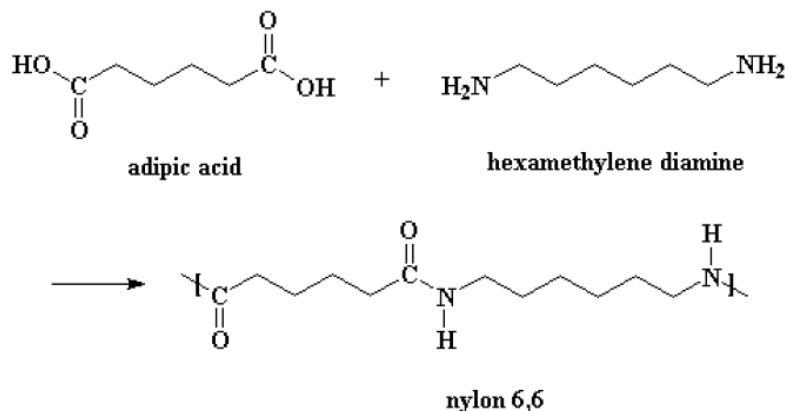
Figure 2 - Example of PA from Two Monomers [10]

Figure 3 shows the resulting general polyamide structures and the naming convention associated with the number of carbons in the chain [7].

$$\text{nylon-}n: \quad -[-(NH-CO)-(-CH_2)_{n-1}-]- \quad (1)$$

$$\text{nylon-}m,n:$$
$$-[-(NH-CO)-(CH_2)_{n-2}-(CO-NH)-(CH_2)_m-]- \quad (2)$$
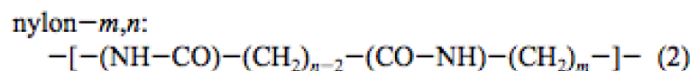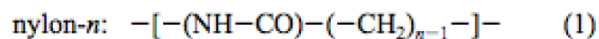
Figure 3 - Polyamide Structure and Naming Convention [11]

For the first type of polyamide, the carbon chains always are attached to an amine and a carboxyl. Because only one monomer is needed, the number of carbons in between the amide bonds is always the same. Therefore, only the one number is required in order to specify the chemical structure. However, for the nylon-*m,n* category, the carbons are surrounded by either one or group or another, rather than both. This allows the carbon chain length to vary between the amines and between the carboxyl groups. This is why two values are required to fully describe the repeating structure of the polyamide. To

6

differentiate between these two different types, some groups refer to nylon *n* and nylon *m,n* as monofunctional and difunctional, respectively [12, 13, 14]. This is not to be confused with the general use of the term functionality in polymers, which refers to the number of functional groups of a monomer as bifunctional or greater [15]. The most common polyamides used in industry are PA 6,6, PA 6,10, PA 6, and PA 11 [16].

2.1.2 Reinforced Polyamide

The concept of reinforcing polymers with filler has been around since the introduction of thermosetting plastics in 1909 [17]. The overall concept is to utilize the valuable structural properties of small fibers by joining them together in a polymer matrix. This allows for the transfer of stress and load to the fibers, while the polymer matrix also distributes this stress across a series of fibre bundles, thus protecting against fibre buckling. This transfer and distribution of stress is crucial to the successful development of a composite.

The primary reinforcing short fiber in the polymer industry is fiberglass. The use of fiberglass dominates the market and is mostly used in a range of 20-40 wt. %, although up to 60% has been reported. Due to the wide use, property data is readily available. Table 2 shows some differences in the properties of neat nylon 6 compared to a composite filled with 30% fiberglass.

Table 2: Properties of Nylon 6 compared with 30% Glass Filled Composite [18]

Property	Neat Nylon 6	30 wt. % Fiberglass
Specific Gravity	1.13	1.4
Tensile Strength	81 MPa	165 MPa
Flexural Strength	113 MPa	193 MPa
Impact Strength	59 J/m	160 J/m

However, despite these improvements in material properties, the use of glass fiber as a filler has the following disadvantages [4]:

1. High density
2. Health and safety issues for human labour
3. Abrasion of processing equipment
4. Complications with recycling

It is due to these issues that alternatives such as wood fibers are considered. These are further discussed in the natural fiber reinforcement section.

2.1.3 Polyamide Blends

Blending of polymers is a widely existing practise used to obtain new materials [19]. The approach is a common method to tailor the properties of a material to achieve a balance between the properties of the original polymers. In most cases, the polymers being combined have very different chemical structures and without additives result in multiple phase morphologies due to being immiscible. Because polyamides have similar structures, it is more likely that the blend will be miscible. A polyamide blend, reported by Chen et al., indicated miscibility of PA 6 in PA 6,6, although the blend also contained nano-fillers and additives [20]. A pure blend of polyamides has been performed by Kiziltas and Lee, in which PA 1010 is successfully combined with PA 6,10 and also with PA 6 [21]. Both of these combinations were designed at 50% weight of each polyamide. However, the similar structure of polyamides, does not guarantee miscibility. The blending of an amorphous aromatic polyamide with various aliphatic nylons produced both miscible and immiscible combinations, as shown in Figure 4 [22].
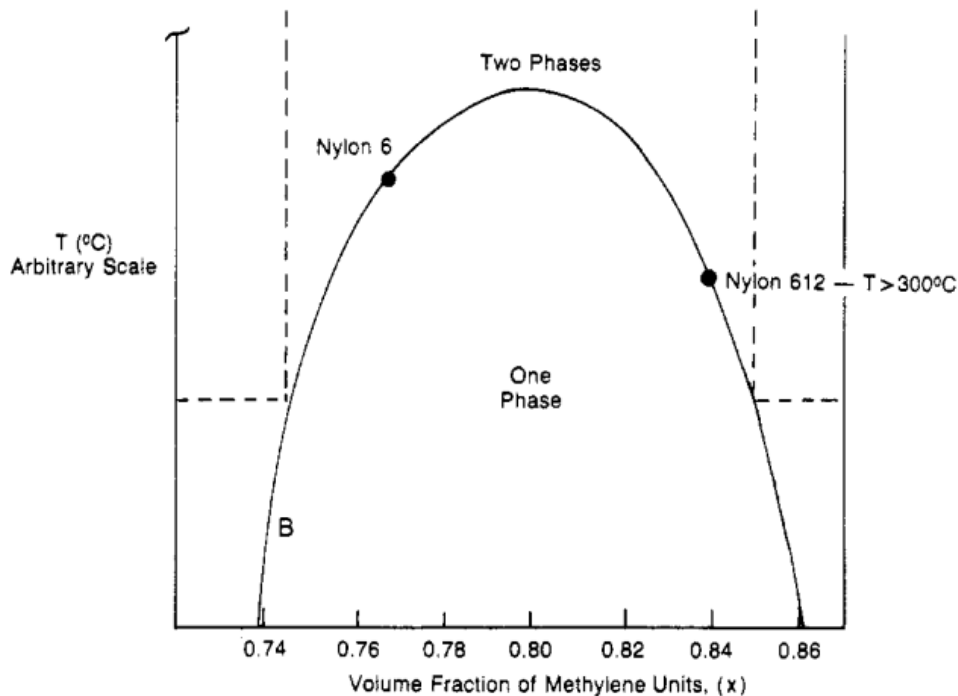
Figure 4 - Aromatic Polyamide Miscibility Figure [22]

Further studies have shown that phase separation is still the dominant behaviour, even for the combination of linear polyamides [23]. However, the combination of PA 6,6 with PA 6 and PA 6,10 is known to be miscible and it commercially applied due to improved processability [24]. Although immiscibility is most common, models suggest that for binary polyamide blends, similar fractions of amide units allow for miscibility [23].

2.2 Wood Fibers

2.2.1 Components

Due to the multitude of applications for the use of wood, wood chemistry is a subject that has been abundantly studied. The three main components of wood are cellulose, hemicellulose, and lignin [25]. The ratio of each of these components is highly dependent on the type of wood and processing history.

9

Cellulose is the main cell wall component, making up to 40-45% of the wood fiber. Linear celluloses chains are stiff and straight which favours the organization of these chains into bundles with crystalline order held by hydrogen bonds. The unorganized chains also exist in disordered amorphous regions.

Hemicellulose consists mostly of sugars other than glucose, although not excluding glucose [26]. The types of sugar present are strongly dependent on the tree type but can be generalized between softwood and hardwood. Softwood trees, also known as evergreens due to the retainment of leaves over the winter, has xylose as the principle sugar making up the hemicellulose. Whereas the hemicellulose of hardwood trees has mannose as its primary sugar structure. Other sugars present include glucose, galactose, arabinose, and rhamnose. The degree of polymerization of hemicellulose is in the range of 100-200, while cellulose is around 7,000-10,000 repeating units [26]. The lower molecular weight and amorphous structure makes hemicellulose more soluble and susceptible to hydrolysis than cellulose [27].

Lignin occurs in wood fiber as approximately 20-30% of the weight composition. It serves as the "matrix" between wood fibers, holding everything together [28]. It also acts as a barrier to enzymatic degradation of the cell wall. Lignin has a very complicated network structure.

2.2.2 Pulping Processes

The method in which wood is refined into compoundable wood fiber has a significant effect on its composition and material properties. There are four general types of pulping processes: chemical, semi-chemical, chemi-mechanical, and mechanical [27]. The two processes relevant to this thesis, based on the wood fibers in consideration, are chemical pulping and mechanical pulping.

Chemical Pulping

Chemical pulping is the process that breaks down the chemical structure of lignin, causing it to become soluble in liquid [27]. A common chemical pulping process is called the Kraft process, which uses sodium hydroxide and sodium sulfide as the chemicals that break down the lignin [29]. In 1996, about 75-80% of pulping in the United States is performed with the Kraft method [27]. The removal of most lignin results in a high strength pulp with only 3-5% lignin content. The pulp yield from this process ranges between 45-70%, depending on how much bleaching is required [27]. Despite chemical recovery methods, chemical pulping remains higher cost compared to mechanical pulping.

Mechanical Pulping

A mechanical puling process repeatedly compresses and decompresses fiber [30]. The most common method disintegrates wood chips between revolving metal disks. High temperature and pressure is used to promote fiber liberation [27]. Because lignin is not removed through any chemical solution, the yield for this process is between 92-96% [27]. However, the strength of the resulting pulp is lower than that of chemical pulping.

2.2.3 Thermal Stability

The thermal decomposition of wood fibers is a complex reaction with unknown mechanisms. At lower-temperature thermal degradation, the decomposition of the material is attributed to the following processes [26]:

1. Reduction in molecular weight
2. Appearance of free radicals
3. Elimination of water
4. Formation of carbonyl, carboxyl, and hydroperoxide groups (especially in air)
5. Evolution of carbon monoxide and carbon dioxide

Concerning pure cellulose, below 200°C it is difficult to distinguish between the effects of temperature accelerating the regular aging reaction versus the onset of thermal degradation [26]. However, above 200 °C, thermal degradation becomes more prominent. Nevertheless, the main weight loss of cellulose does not occur until 315-400 °C [31].

2.3 Natural Fiber Reinforcement

2.3.1 Incentives and Disadvantages

Wood and natural fiber filled composites have been quite successful replacements over traditional reinforcing fillers such as glass fibers and talc fillers. Fiber reinforcement of thermoplastic polymers is known to improve tensile and flexural modulus and strength while negatively affecting ductility and impact resistance [32]. Not only can this reduce the overall cost of plastic components, but it can also add value to an agricultural product [33]. Some advantages of natural fibers include [34, 35]:

1. Being renewable
2. Low Cost
3. Low density
4. Safe processing
5. Recyclable at the end of the product life

Because natural fibers are grown, they act as carbon storage, thus reducing the carbon footprint of a composite part. Additionally, the low cost and low density (compared to glass) simultaneously reduces price and weight of the material. The use of natural fibers in processing is not hazardous to workers or abrasive to the process equipment, as is the case with glass fibers. This introduces more cost savings as mitigation of hazards is not necessary and the equipment would last longer. However, there are also some challenges that may arise with the use of natural fiber in general:

1. Seasonal production limitations
2. Availability globally varies
3. Nonhomogeneous properties
4. Poor thermal stability
5. High moisture absorbance

These disadvantages need to be addressed in order to achieve a commercially viable product. Other applications for wood fiber have already addressed some of these issues. For example, the paper industry is capable of handling the seasonal growth schedule and producing a uniform, quality product. Wood pulp is a global commodity. The issue of thermal degradation remains a challenge because the high processing temperatures during manufacturing nylon parts can induce degradation reactions which results in voids occurring in the composite [36]. These voids negatively impact mechanical properties due to poor stress transfer [37, 38, 39]. Additionally, voids in a composite are potential failure initiators and can propagate crack growth [38].

2.3.2 Previous Work

The use of cellulose fiber as a filler in nylon has been considerably investigated in the past. In 1984, Klason et al. observed that cellulose fillers in PA 6 increased elastic modulus but decreased strength and elongation. A considerable darkening of the composite was also observed due to chemical degradation [40]. A study by Sears et al. has compared a variety of wood cellulose pulps in a PA 6 matrix and found that the best results come from the higher cellulose purity pulps [41]. Xu has performed an extensive study on cellulose in both PA 6 and PA 6,6, looking at effects of molding procedure, processing temperature, and thermal degradation [34]. Other natural fibers have also been considered such as wheat straw [4, 36], kenaf, flax and hemp [42]. A recent study by Kiziltas et al. has investigated the use of microcrystalline cellulose in PA 6 [43, 44]. Similar to this study, Kiziltas et al. investigates cellulose filler in blends of PA 10,10 with PA 6 and PA 6,10 [21].

Many studies have used various means of reducing the polyamide melt temperature in an effort to mitigate thermal degradation. Misra et al. lowered the melt temperature of PA 6 with three percent lithium chloride salt. This reduced the melt temperature by 24 °C and resulted in an increase of tensile modulus and strength using hemp fibers [45]. Another study used a combination of lithium chloride salt as well as a plasticizer to reduce the melt temperature for a composite containing wheat straw [4].

Without changing melt temperature, Sears et al. published a patent that changed the extrusion process to minimize temperature, thus giving the degradation less energy to proceed. They proposed an extrusion with initial temperatures just slightly above the melting temperature of the polyamide and then lower intermediate temperatures as the shear heating would maintain the melted state of the polyamide without needing the additional heating from the extruder. This resulted in cellulose composites with reduced discoloration [46].

Another approach taken to reduce thermal degradation is to try to increase the thermal stability of the natural fiber. A study by Vedoy shows increase of the onset of thermal degradation through silane modification and exposure to ultraviolet light [36]. The use of ultraviolet light is discussed more in the next section.

2.4 Ultraviolet Light Treatment

The use of ultraviolet light to improve thermal stability is a new approach used by Vedoy in the study of wheat straw fibers. It is reported that, for wheat straw fibers, 15 minutes of exposure to high power UV irradiation increases the temperature at which 2% of weight is lost by 50 °C [36]. Studies of UV effects on wood suggest that the UV irradiation alters or removes the lignin and hemicellulose present in natural fibers through complex photochemical reactions [47]. It is also reported that long-term UV exposure significantly reduces the amount of lignin present in wood [48].

2.5 Carbon Fiber

Modern carbon fiber was developed in the 1970s for use in aerospace industry [49]. However, the high cost kept its application limited to aerospace and high-end sporting goods. Carbon fiber is considered the most promising candidate for future lightweight materials due to its high stiffness and strength combined with the low density of the fiber backbone. However, the high cost prevents the commercial use in cost competitive applications. Even though it is currently not an economical option, a comparison of carbon fiber development history to that of glass fiber indicates that there is potential for technological improvements to allow for feasibility in the future [50].

A study by Karsli and Aytac, demonstrated the increase of mechanical properties of PA 6 as carbon fibers were added, up to 20 percent [51]. Figure 5, below, demonstrates the increase in modulus and also shows that initial fiber length did not affect the modulus.
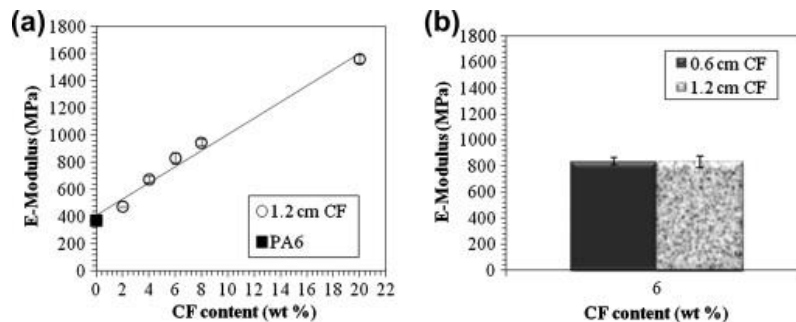
Figure 5 - Tensile Modulus of Nylon 6 and Carbon Fiber Composites [51]

The steady modulus in part B of Figure 5 is due to fiber breakage during the extrusion and injection moulding process. Increased fiber filling leads to more interaction, which causes breakage of the fibers. This leads to initial size differences of the fibers having less effect on the material properties [52].

3. 0 Experimental

3.1 Materials

3.1.1 Polyamides

Industrial partners supplied the polyamides (PA) used in this research. The recycled PA 6 was kindly supplied in the form of pellets from Wellman Plastics Recycling, LLC. Differential scanning calorimetry (DSC) and scanning electron microscopy (SEM) analysis showed that there are small amounts of another material identified as polypropylene existing in the recycled PA 6. The PA 6,10 and PA10,10 were obtained from Vestamid by Evonik Industries. The PA 6,10 is 62% renewable, while PA 10,10 is 100% renewable (bio-based). Product specifications can be found in Appendix A.

3.1.2 Wood Fibers

The wood fibers and cellulose were supplied from three commercial companies. Woodforce provided two generations of wood fiber pellets, referred to in this thesis as Woodforce 1 and Woodforce 2. The difference between these two generations is unknown as the supplier did not disclose it. These fibers are known to be mechanically pulped and come in the form of square pellets, as shown in Figure 6.

Figure 6 - Woodforce Fiber Appearance

The second wood fiber used in this research was produced by Suzano Pulp and Paper Company. The pulp produced by Suzano is from eucalyptus trees and is chemically pulped by the Kraft process and bleached. It was provided in the form of pulp sheets and it was ground up before being extruded. The ground fiber had a consistency very similar to cotton balls.

CreaFill Fibers Corp. provided the cellulose used in this research. The product name is CreaTech TC 200. Average fiber size is 155 micron length, 20 micron width, and 1-2 micron thickness. Cellulose content is 99.6% dry base minimum. Figure 7 shows an image of the CreaTech TC 200. Material data is provided in Appendix A.

Figure 7 - CreaFill Cellulose Appearance

3.1.3 Carbon Fiber

The carbon fiber used in this project is provided by Toho Tenax. A milled short fiber was used with average length of 100 microns. Due to delays, there was limited quantity of available product to perform experiments. Further material specifications are provided in Appendix A.

3.1.4 RP 17

RP17 is a process additive for reducing material odor. RP17 is a commercial formula produced by Struktol. It is an odor-neutralizing agent commonly used in polyethylene and polypropylene products. The technical data for this product is provided in Appendix A.

3.2 Procedures

3.2.1 Thermal stability

Thermal gravimetric analysis (TGA) of the natural fibers was performed using TA Instrument's TGA Q500. A starting weight of 8-12 mg of fiber is heated from 25°C to 600°C at heating rates varying from 5°C/min to 50°C/min. These heating conditions were performed under nitrogen and air environments at a flow rate of 30 mL/min. Reaction kinetics are evaluated through the variation of rates. The TGA data was used to measure the thermal stability by calculating temperature of thermal degradation and activation energy.

TGA of composites was performed on a Mettler Toledo analyzer on samples of about 10 mg. Samples were created by cutting up extra injection moulded bars into small chips, approximately 2-3 mg each. These chips were obtained from multiple locations from multiple bars in order to minimize possible effects of poor distribution. Each sample was scanned from 25 °C to 600 °C at a heating rate of 10 °C/min under nitrogen with a flow rate of 30 mL/min to avoid sample oxidation.

3.2.2 Melting Point and Crystallinity

Differential scanning calorimetry (DSC) was performed on a Mettler Toledo Differential Scanning Calorimeter. Samples were prepared at approximately 10 mg weight, in a similar fashion to the TGA sample preparation. The sample was first heated from 25 °C to 300 °C at a rate of 20 °C/min to remove any thermal history, then held at 300 °C for 5 min, cooled from 300 °C to 0 C at a rate of -10 °C/min, held at 0 C for 5 min, and heated again to 300 °C at 10 °C/min.

The DSC data was used to calculate melting and crystallization temperatures and crystallinity. For a pure polymer, Equation 1 describes how the weight fraction of crystallinity would be calculated [53].

$$X_c = \frac{\Delta H_f}{\Delta H_f^\circ} \tag{1}$$

In the above equation, ΔH_f is the measured melt or crystallization enthalpy and ΔH_f° is the reference heat of fusion for a 100% crystalline structure. Table 3 lists the specific reference values used for calculations of crystallinity [54].

Table 3: Reference of 100% Crystalline Heat of Fusion [54]

Polymer	$\Delta \widehat{H}_f^\circ$ (J/g)
PA 6	230
PA 610	254
PP	207

Because the enthalpies measured are based on the full weight of the specimen, an adjustment to Equation 1 is needed to account for the weight of the composite that does not contribute to the crystallization. For the case of the polypropylene phase, the enthalpy can be divided by the estimated mass fraction of polypropylene to obtain Equation 2.

$$X_{c_{PP}} = \frac{\Delta \widehat{H}_{f_{PP}}}{\mathrm{m_{PP}} \Delta \widehat{H}_{f_{PP}}^\circ} \tag{2}$$

For the polyamide phase, there is only one observable peak to account for the two types of polyamides crystallizing. Thus, in addition to the adjustment for mass fraction, the reference enthalpies of fusion are weighted based on the mass fractions present. Equation 3 describes the calculations used for the polyamide phase. Appendix C describes further how these equations are obtained.

$$X_{c_{PA}} = \frac{\Delta \widehat{H}_{f_{PA}}}{m_{PA610} \Delta H_{f_{PA610}}^\circ + m_{PA6} \Delta H_{f_{PA6}}^\circ} \tag{3}$$

These equations are used to calculate the fractions of crystallinity within the polypropylene and polyamide phases, respectively.

3.2.3 Morphology and Size

Scanning electron microscopy (SEM) was applied to capture images of composite surfaces. The machine used is a JEOL 6610 SEM. The surfaces studies were fractured from the notched Izod impact tests. Surfaces were carbon coated prior to SEM imaging. The micrograph images were used to evaluate the morphology of the samples, size and distribution of phase.

3.2.4 Compounding

The first set of composites was extruded using a MiniLab Extruder Haake produced by Thermo Electron Corporation. Both, fibers and polyamide, were reduced to smaller size before extrusion using a Retsch ZM 200 centrifugal mill. A two-millimeter sieve was used to reduce the side of the polyamide pellets and a one-millimeter sieve was used for the fibers. The size reduction of the PA pellets and fibers allowed for better mixing and dispersion prior to getting extruded. After being ground, material was dried overnight in a vacuum oven at 50 ℃. The extruder temperature was set to 240 ℃ with a screw speed of 60 RPM.

The second set of composites was extruded using a ThermoHaake Rheomex twin-screw extruder. All material extruded was dried overnight in an oven at 70℃. Maximum screw temperature is 230 °C at the screw tip, with zones reduced by 5 ℃ every two zones such that the first zone is 215 ℃, as described in Table 4. Screw speed is controlled manually but approximated to be 120 RPM. All samples were extruded twice in order to ensure even distribution of cellulose and polyamide.

Table 4: Extruder Temperature Profile

Zone	1	2	3	4	5	6	7	Tip/die
T (℃)	215	215	220	220	225	225	230	230

3.2.5 Injection Molding

The first set of composites was injection molded using a Ray-Ran RR/TSMP. Extruded samples were cut into segments less than 20 mm in length. These were dried in a vacuum oven overnight. Extruded pellets were placed in the barrel of the injection molder and left for approximately 10 minutes to heat up. The barrel temperature was set at 240 ℃ and the mould plates were set at 80 ℃. Pressure applied was approximately 100 psi.

The second set of composites were then injection molded using a Boy 80M injection molder at a maximum temperature of 246 °C. The initial temperature zone was set at 237℃ and was gradually raised to 246℃ at the injection point. Max pressure was set to 1,000 psi. The mould temperature was approximately 85℃. Compounded material was dried overnight and kept in the oven until immediately before injection. Each shot would produce an ASTM standard Type-I tensile dumbbell and flexural bar samples.

3.2.6 Mechanical Properties

The first set of composites underwent three-point bending flexural tests using a TestResources Inc. 120Q1000 machine. Flexural properties were determined according to ASTM D790-10 procedure A. The test samples were kept at 50% relative humidity for a minimum of two days after being injection molded before being tested.

The second set of mechanical tests was performed after one week of samples being at 23ºC±2 and 50%±5 relative humidity. Tensile and flexural tests were carried out using an Instron 3366, adhering to ASTM D 638-10 and ASTM D 790-10, respectively. For tensile testing, ASTM Type I bars were tested at a rate of 5 mm/min. The Instron was equipped with a 5-kN load cell and a travel extensometer. Flexural tests were performed using ASTM Procedure A at 1 mm/min up to 5% strain. At least six samples per loading level were tested for tensile and flexural properties.

All Izod impact testing were conducted according to ASTM D256. A 10 pound pendulum was used to hit the notched sample on a Testing Machines Inc. Model 43-02

impact test machine. The first set of samples tested 5-8 samples per composition while the second set was adjusted such that 10-12 samples were tested for impact properties due to high levels of deviation.

3.2.7 Ultraviolet Treatment

Wood fibers were exposed to ultraviolet (UV) light for the duration of 15 minutes. Fibers were ground using the Retsch ZM 200 centrifugal mill with a sieve of 1 mm. Approximately 50 mg of fiber was spread over an aluminum dish. The custom built UV radiation system used a 1.8 kW UV light source. The spectral output of this light is shown in Figure 8.
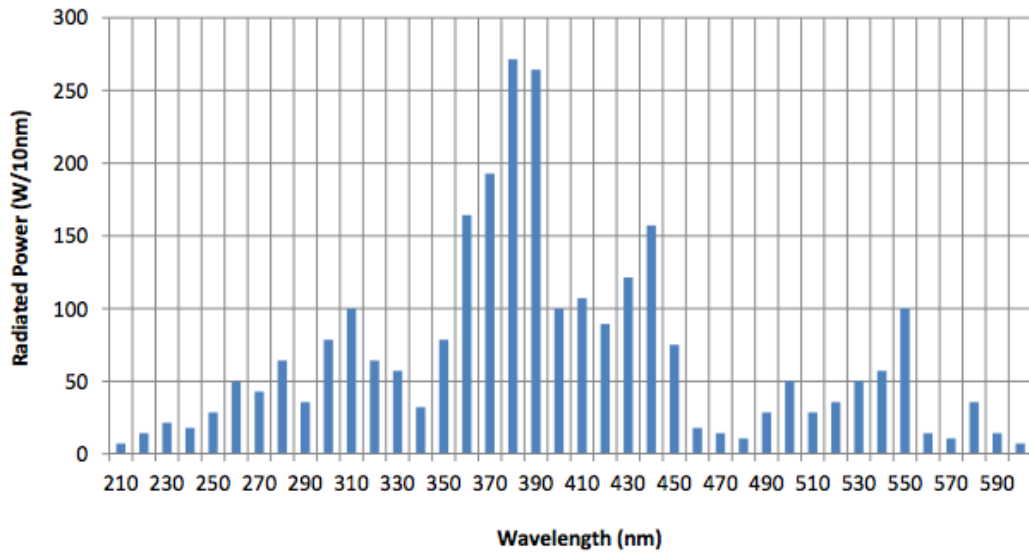
*Figure 8 - UV Light Spectral Output *Reference*: Fusion Systems Inc*

4.0 Thermal Stability of Wood Fibers

4.1 Introduction

To begin this research, the wood fibres, Woodforce 1, Woodforce 2, and Suzano fiber are compared prior to compounding with polyamide. A thermal analysis is performed to compare thermal properties before the extrusion process. Using a range of heating rates allowed the calculation of thermal degradation kinetics. Also compared, is the temperatures at which the fibers have lost 5 wt-% of their initial weight, referred to as $T_{5\%}$. An isothermal test is run at 250°C because this is the general processing temperature of nylons in industry. Finally, fibers exposed to UV light for the duration of 15 minutes are compared to the unexposed fibers for changes in thermal stability.

4.2 Results and Discussion

4.2.1 Weight Loss vs. Heating Rate

Figure 9 shows the TGA curve trend over the range of heating rates used. It can be seen that the curves are all very similar with an offset in the drop of sample weight by temperature. This offset is consistently in order of heating rate for all fibers observed. The shift in the curve to the right is attributed to higher heating rates. At the widest range of temperature difference, there is approximately a 50°C difference in the temperature in which the Suzano fiber reaches 50 wt-% of its original weight when comparing the heating rates of 5°C/min and 25°C/min.
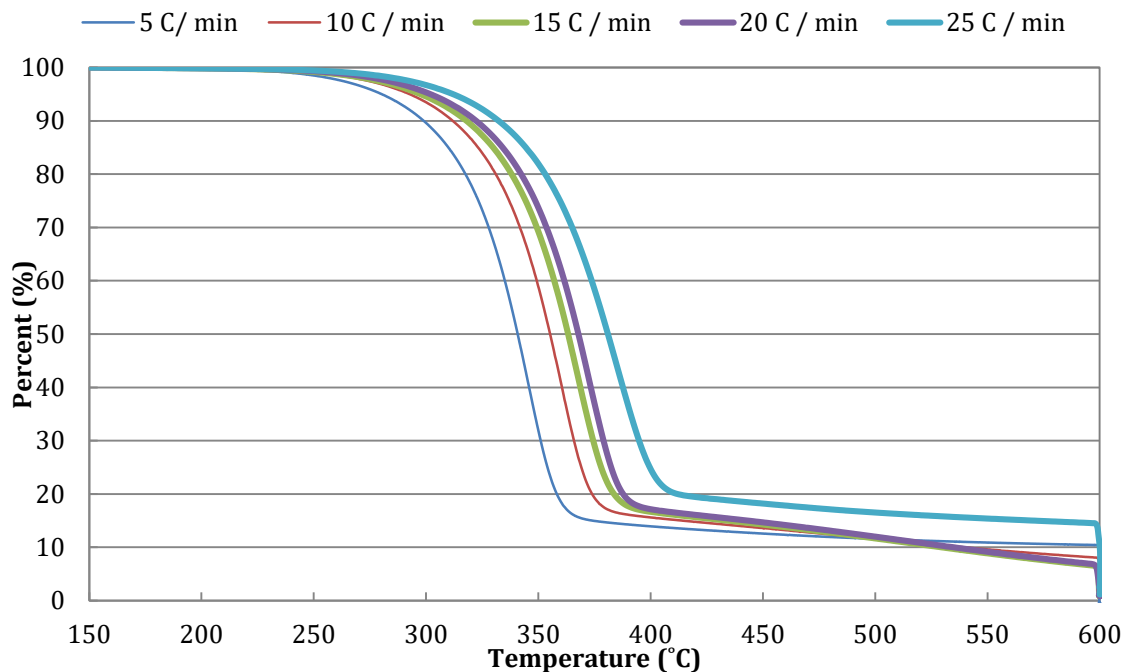
Figure 9 - Suzano Nitrogen TGA Curves

The observed curve shift is expected due to the limited control over the heating environment. The thermocouple inside the TGA instrument cannot account for heat transfer within the fiber sample. Additionally, a slower rate of temperature increase allows for more time for the thermal degradation reaction to progress.

For each heating rate, the temperature at which the fiber has lost five percent of its initial weight is shown in Figure 10. It can be observed that the Suzano fiber has the higher $T_{5\%}$ values for each heating rate followed by WF2 fibers in the middle and WF1 having the lowest values. There is also an increase in temperature when comparing samples that were heated in nitrogen as opposed to those heated in air.
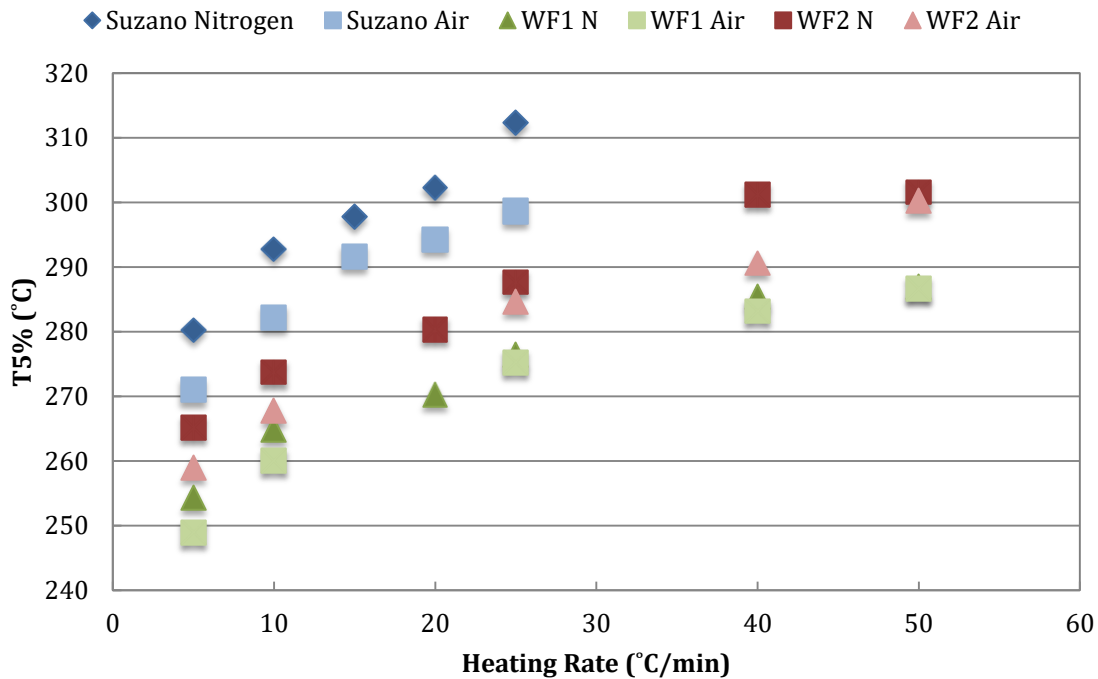
Figure 10 – Thermal stability measured as temperature to reach 5 wt.% loss vs. heating rate

The higher $T_{5\%}$ values of the Suzano fibers implies that it can withstand exposure to higher temperatures with less thermal degradation than the Woodforce fibers. This is due to the Suzano fibers having more cellulose content compared to the Woodforce fibers. Additionally, the second generation of Woodforce demonstrates higher temperature tolerance than the first generation. The differences between the air and nitrogen environments indicates that the reactions occurring for the Suzano fibers relies more on the presence of oxygen than that of the Woodforce fibers, which have a much smaller difference when comparing $T_{5\%}$ values between environments.

4.2.2 Kinetics of Thermal Degradation

Determination of the activation energy of the thermal degradation is calculated using the ASTM standard E1641 – 13 [55]. This method is based on the isoconversional Ozawa-Flynn-Wall method. This method is selected because it does not assume a certain

specific reaction mechanism and has been used in literature to report kinetic parameters of various natural fibers [56].

The fundamental rate equation that the method is based on is given in Equation 4.

$$\frac{d\alpha}{dt} = k(T)f(\alpha) \qquad [4]$$

This states that the rate of thermal degradation ($d\alpha/dt$) is a function of temperature (T) and conversion (α). The conversion (α) used in this analysis is calculated as shown in Equation 5.

$$\alpha = \frac{w_{initial} - w}{w_{initial} - w_{final}} \qquad [5]$$

The initial weight (100 wt-%) is taken at 150°C to remove the effect of moisture; this procedure was applied to all samples discussed in this document. The final weight is taken at the point in which the TGA curve plateaus. The selection of these points is performed visually due to the curves not fully plateauing and undergoing secondary drops in weight. Figure 11 shows the occurrence of a secondary drop that occurs when the sample is heated under an air environment.
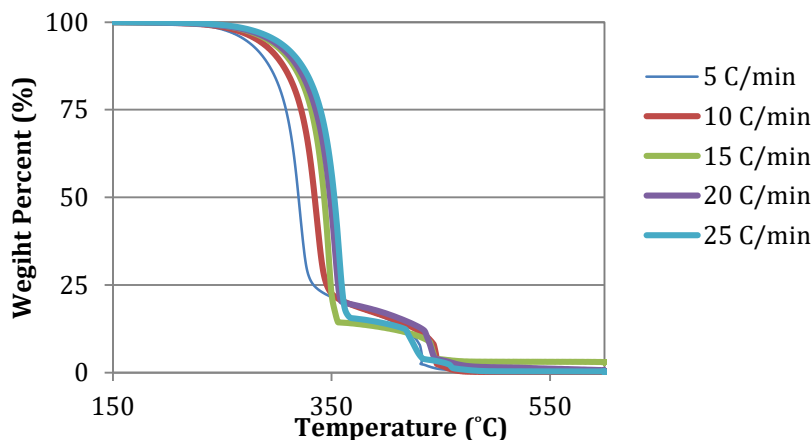
Figure 11 - TGA Curve of Suzano Fiber in Air as Example of Curve Shape

The secondary thermal degradation is ignored in these calculations due to the onset temperature range being higher than expected processing conditions.

The dependence of the reaction rate to temperature is described by the Arrhenius equation, given in Equation 6.

$$k(T) = A\exp\left(-\frac{E_a}{RT}\right) \qquad [6]$$

Additionally, the rate equation is transformed to change with temperature by dividing both sides by the heating rate (β). This can be done because the heating rate is constant throughout the entire TGA curve. This results in Equation 7.

$$\frac{d\alpha}{dT} = \frac{A}{\beta}\exp\left(-\frac{E_a}{RT}\right)f(\alpha) \qquad [7]$$

This equation is then integrated numerically and results in a linear relation between the log of the heating rate versus the reciprocal of temperature at a desired conversion amount. Plotting $\log(\beta)$ versus $(1/T)$ results in a linear relation in which that slope may be used to calculate activation energy according to Equation 8. Many functions exist for the approximation of the integral with respect to temperature. The approximation function used by the ASTM standard used a table of integration constants that provide the variable b and Equation 8, below.

$$E_a = -\frac{R}{b} \times slope \qquad [8]$$

The ASTM standard recommends using a conversion of 5 wt-% but requires that any amount chosen must be below 20 wt-%. In this analysis, 3 conversions were selected in order for comparison of values. These conversions are 5, 10 and 15 wt-%. Note that this approach considers the change in weight (wt-%) measured by TGA as an approximation of chemical conversion assuming that the result of thermal degradation are volatile products. Table 5 lists the calculated activation energies for each conversion.

Table 5: Activation Energy of Fibers

Conversion		Activation Energy (kJ/mol)		
		5%	10%	15%
Air	Suzano	125.0	122.3	123.6
	WF 1	135.9	143.4	149.3
	WF 2	136.6	132.5	129.2
Nitrogen	Suzano	141.5	141.2	143.2
	WF 1	162.2	164.2	166.5
	WF 2	138.4	139.8	143.4

Figure 12 and Figure 13, below, graph the calculated values of activation energy found for each fiber using conversion values of 5 wt-%, 10 wt-%, and 15 wt-%. Figure 12 refers to the thermal kinetics when measured in an air environment whereas Figure 13 is in an inert environment. A higher activation energy is observed for the nitrogen environment, as compared to in air. For both figures, Woodforce 1 has the highest activation energy while Suzano fibers have the lowest.
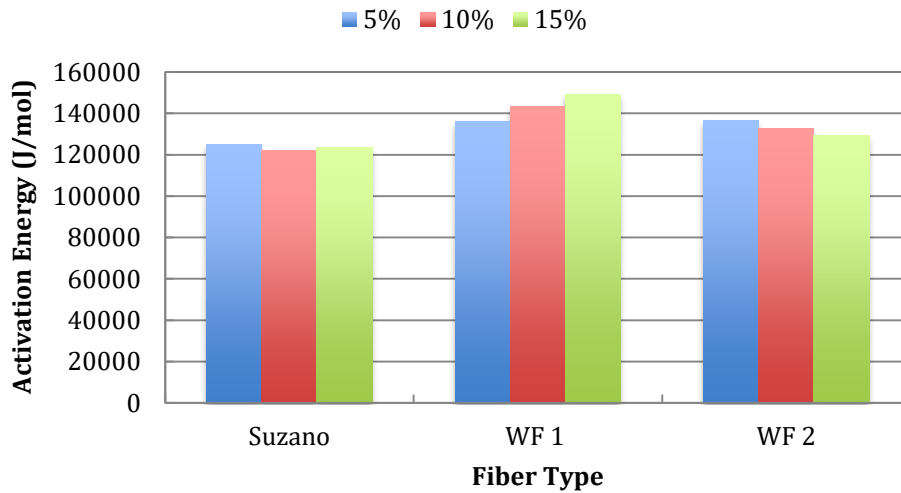
Figure 12 – Fiber Degradation Kinetics in Air: Activation Energy
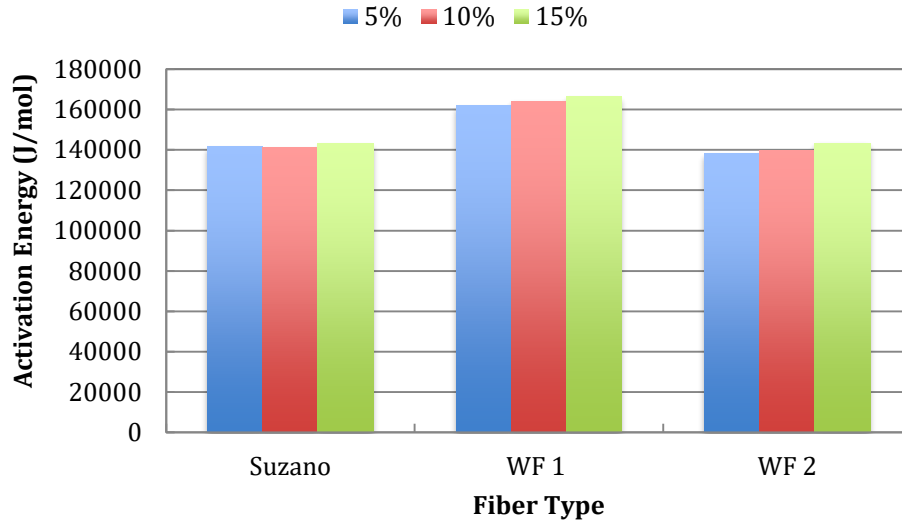
Figure 13 - Fiber Degradation Kinetics in Nitrogen: Activation Energy

Based on Equation 7, a higher values of activation energy would result in a slower reaction rate. Slower reactions would be expected to be more thermally stable because it would take more time for the thermal degradation to occur. However, these results do not correspond to what has been observed previously when compared to the $T_{5\%}$ values. Instead, we have the highest values of activation energy as Woodforce 1, which has the lowest $T_{5\%}$ temperatures. The main difference between these two comparisons is that the thermal kinetics analysis takes into consideration a variety of heating rates. This suggests that the way heating rate affects the thermal degradation would favor Woodforce 1, possibly, through how the composition transfers heat. The TGA curves used in these calculations are plotted for reference in Appendix D.

4.2.3 Isothermal TGA

During the compounding and extrusion processes used in the production of composite parts, the fibers will be exposed to and held at approximately 250°C. The processing temperatures for PA may vary according to material and equipment. The temperature of 250 °C is considered here a reference polyamide processing temperature [36]. For discussion purposes, an isothermal test was run to compare fiber weight lost at

this temperature over time. Figure 14 shows the resulting isothermal curves at this condition. Similar to the non-isothermal results, it is apparent that Suzano fiber experiences less weight loss than the Woodforce fibers. Woodforce 1 experiences the most weight reduction.
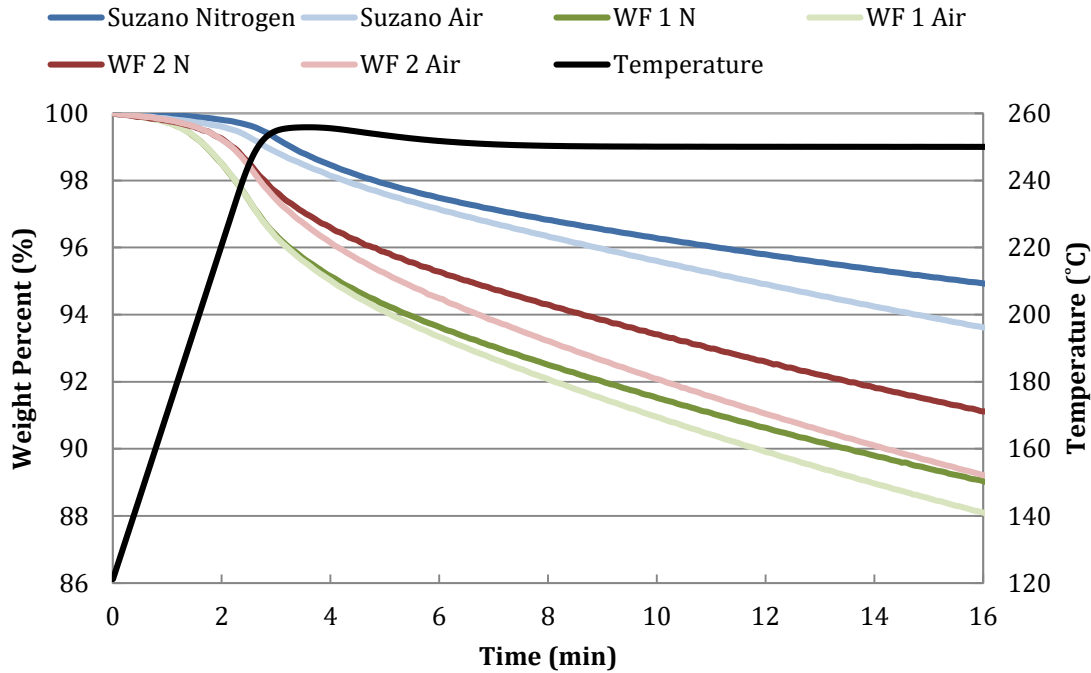
Figure 14 - Isothermal TGA at 250 ˚C

Over the amount of time measured, the most weight lost did not exceed 12 weight percent of the original fiber. The measurement was limited to 16 minutes because this is representation of cycle times in automotive parts manufacturing. It is likely that the cycle time will be in the order of few minutes.

Due to the weight loss by products being gaseous, any small amount of thermal degradation could result in a significant volume of void formation inside of a composite material. The curves in Figure 14 have three stages:

- Stage 1 – Heating: time approximately initial 2 minutes, this stage has minimal weight loss, it may include drying of any moisture that could have been absorbed by the sample during handling (samples were dried prior to analysis)
- Stage 2 – Transition: time approximately 1-2 minutes, this is the onset of thermal degradation, it is characterized by maximum slope (negative slope) indicating the maximum rate of thermal degradation
- Stage 3 – Continuous Degradation: this stage starts with an inflexion in the curve after the transition stage, the rate of thermal degradation decreased significantly and tends to steady-state, almost linear.

It demonstrates the importance in minimizing the amount of time that fibers are exposed to high temperatures. Although compounding and injection moulding procedure is not within the scope of this thesis, minimization of natural fiber residence time would greatly improve the success of natural fiber composites. Additionally, the presence of air is shown to reduce the fiber weight more quickly. If the isothermal parts of the curves could be approximated as lines, the slopes of the fibers in air are consistently steeper. This indicates an even greater dependence on the residence time of the fiber at high temperatures. If the processes could be performed in an inert atmosphere, such as nitrogen, the thermal degradation would be reduced.

4.2.4 UV results

Previous research in our laboratory by Vedoy has shown significant improvement to thermal stability by exposure of natural fibers to ultraviolet light [36]; the thermal stability of straw fibers was improved significantly by exposure of those fibers to UV light. A similar method was used here in an attempt to improve the thermal stability of wood fibers. Figure 15 depicts the resulting non-isothermal TGA cures measured with a heating rate of 20°C / min with and without UV treatment
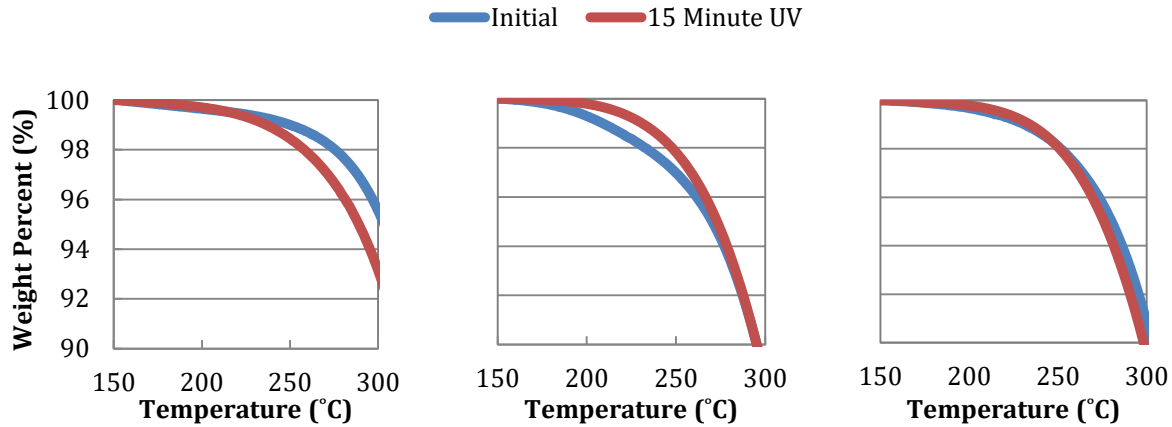
Figure 15 - TGA Curves for Fibers after 15 minutes of UV treatment. Left: Suzano, Middle: WF1, Right: WF2

The left graph in Figure 15, which corresponds to the Suzano fiber, has the UV treated fiber curve consistently lower than the untreated curve. This would imply that the UV treated sample lost more weight and thus demonstrated lower thermal stability. However, in the middle graph, referring to Woodforce 1, the UV treatment is shown to successfully increase the temperature at which thermal degradation occurs. For Woodforce 2, the curves are very similar. Initially, it would appear that the UV treatment very slightly improved weight retention, however, at higher temperatures, the non-treated fiber curve is slightly higher.

Figure 16, below, graphs the $T_{5\%}$ values of the UV treated sample onto Figure 10. Similar to what was observed from Figure 15, the $T_{5\%}$ value is reduced for Suzano fiber and increased for Woodforce 1 while Woodforce 2 shows a slight decrease.
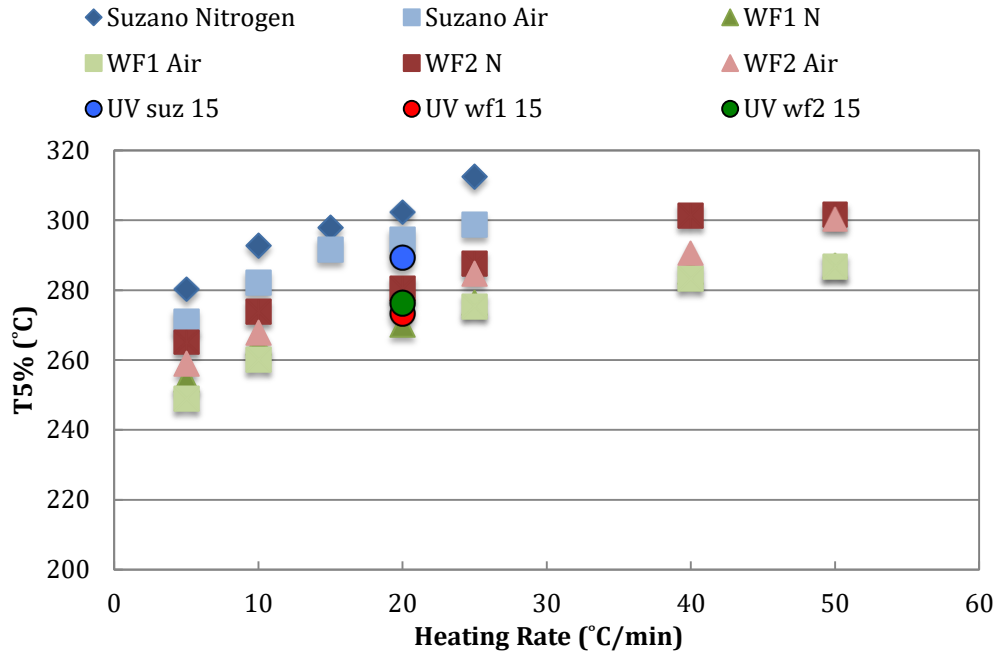
Figure 16 - 5% Weight Loss Temperatures vs. Heating Rate with UV treated Fibers

The varying results of the UV treatment can be contributed to the varying compositions of the wood fibers. Other studies suggest that the effect of UV light mainly alters the lignin present in the fibers [48, 47]. Because Woodforce 1 has the most lignin, it is the most improved by the UV treatment. However, as the Suzano fiber has a small amount of lignin content, there is no positive effect from the UV treatment. Moreover, from the increased deterioration, there may be indication of the UV treatment negatively impacting cellulose thermal stability. The Woodforce 2 curve in Figure 15 confirms this trend as the lower temperature indicates where lignin would thermally degrade while higher temperatures are affected by cellulose. It can be concluded that the UV treatment would be beneficial to mechanically pulped wood fibers.

5.0 Initial Fiber and Polyamide Compounding

5.1 Introduction

After investigating the thermal behaviour of the wood fibers individually, compounding at 20 weight percent filler was performed to evaluate how the fibers affect the flexural and impact properties. Further investigation of the Suzano fiber and Woodforce 2 fiber was performed at levels of 20 and 30 weight percent of fiber in the composite. Each fiber was compounded with PA 6,10, PA 10,10 and recycled PA 6.

5.2 Results and Discussion

5.2.1 Twenty Percent Fiber Content

While extruding the fiber and polyamide compositions, there was moderate difficulty feeding the fibers into the extruder. While neat polyamide will easily be fed via the attached mechanical device, the addition of fiber required manual pushing into the screw-section.

The resulting product had visual evidence of colour change (thermal degradation). The Suzano fiber, which is initially white, resulted in a medium brown colour. The Woodforce fibers, which are initially brown, resulted in a dark brown colour. After injection moulding, all composites were visually dark brown, almost black.

Figure 17 and Figure 18 depict the flexural modulus and strength of the composites. A very similar trend is observed in comparing Figure 17 and Figure 18. In general, the flexural strength and modulus is increased for each polyamide with the addition of the twenty percent natural fiber.
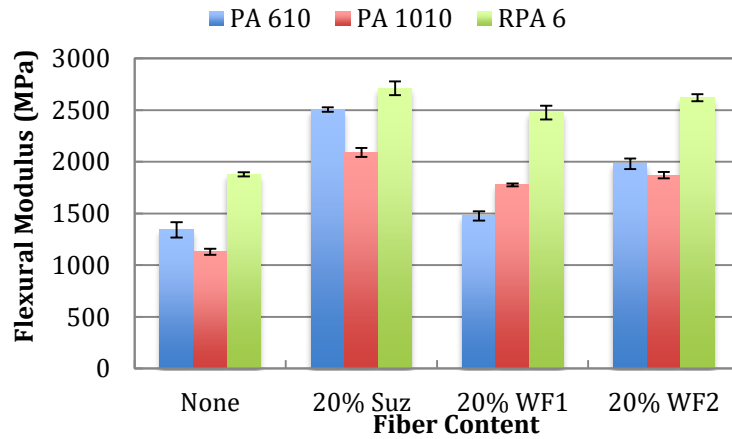
Figure 17 - 20% Fiber content Flexural Modulus
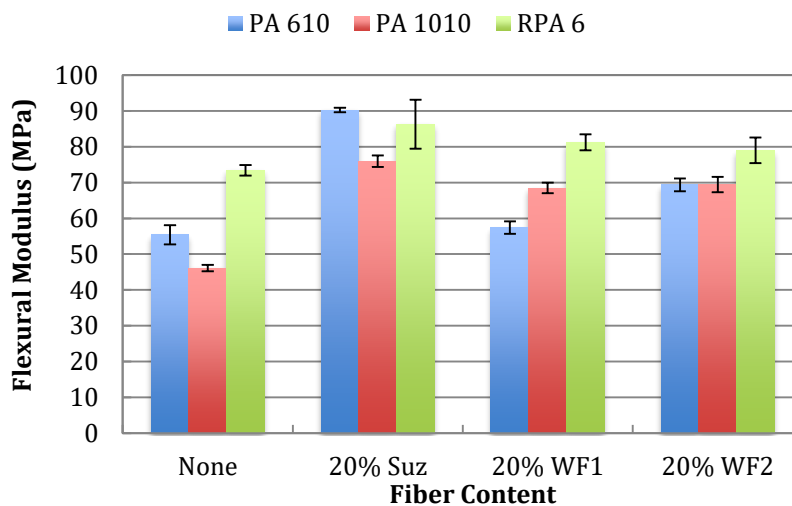
Figure 18 - 20% Fiber content Flexural Strength

The largest increase in flexural properties is observed with the addition of the Suzano fiber. Recycled polyamide 6 shows higher property values, however, relative change is more significant for PA 6,10 and PA 10,10.

The notched Izod impact properties of the same composites is graphed in Figure 19. Contrarily to the flexural properties, impact strength is shown to decrease with the addition of fibers.
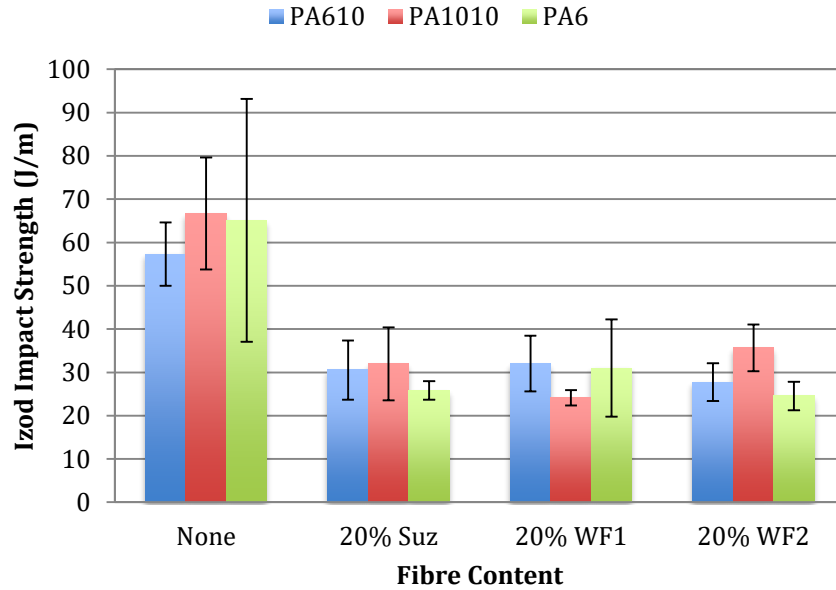
Figure 19 - 20% Fiber content Izod Impact Strength

Although the fiber content does reduce impact strength, the difference between types of fiber cannot be compared. This is because the variance of this test is relatively high. Table 6 shows the analysis of variance of impact strength for the 20% composites. Due to the f-statistic values being lower than the critical values, it can be concluded, with 95% confidence, that there is no statistically significant difference. This is true both for fiber type and polyamide type. The primary observation gained from Figure 19 is that the addition of 20% natural fiber content reduces the impact strength, approximately by half.

Table 6: ANOVA Table for Impact Strength versus Fiber and Polyamide Type

Source	DF	SS	MS	F	$F_{crit}(\alpha = 0.05)$
Polyamide	2	216	108	2.70	3.23
Fiber	2	1.72	0.86	0.02	3.23
Interaction	4	463	116	2.89	2.60
Error	41	1642	40.1		
Total	49	2324			

5.2.2 Added filler level for Suzano Fiber and Woodforce 2

Based on the results found in the initial investigation, it is determined that the first generation of Woodforce fibers consistently has lower property values than Woodforce 2, and therefore, is excluded from further investigation. For more perspective on the effect of filler content, another level of filler is added to the test compositions. The same tests are performed again with the addition of a 30% fiber level and the exclusion of Woodforce 1.

For the lab-scale twin screw extruder used, compounding with 30% fiber content in one step created difficulties in feeding the extruder. The difficulty is associated with the low bulk density of the wood fibers as prepared here. With the procedure used, 30% would be considered the highest possible level in one compounding instance due to the high bulk volume of the fibers. Because the fibers are not intended to melt, enough polyamide needs to be present as it gets fed in order to pickup to fiber and carry it through the extrusion process. It is possible that higher levels could be achieved through multiple extrusion processes, however, this would significantly increase the amount of time that fibers are exposed to high temperatures.

Figure 20 shows the flexural modulus of the second set of samples. For both, Suzano fiber and Woodforce 2, the flexural modulus significantly increases as the filler content is increased from 20 to 30 percent.
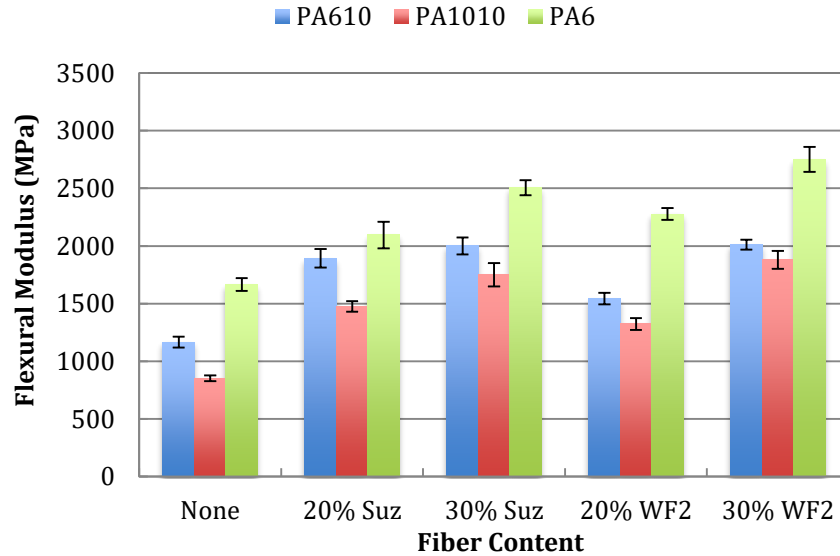
Figure 20 – 20% and 30% Fiber content Flexural Modulus

In contrast to Figure 17, the Woodforce 2 composite values are closer to and sometimes higher than the corresponding Suzano fibers. A closer comparison of the values led to a variety of statistical comparisons with ANOVA tables reported in Appendix B. The strongest correlation observed in these tables is the relation between the polyamide type and the flexural modulus. Therefore, the variation between polyamides needs to be accounted for before comparison can be made between filler level and fiber type. Thus, the ANOVA tables are set up with two-factor levels to separate the influence of polyamide types. Comparison of Suzano fiber and Woodforce 2 fiber shows that, overall, the Woodforce fiber has a slightly higher flexural modulus. However, at the 20% filler level, the statistical difference is not significant, while at 30%, it is. At the 20% level, the interaction between polyamide and fiber is significant, indicating that the differences are significant but depend on the polyamide. For example, in Figure 20, PA 6,10 and PA10,10 show higher flexural modulus for Suzano fiber, while PA 6 shows a higher flexural modulus with Woodforce 2. Between filler levels, there is statistically verified increase in modulus from 20% to 30% for both fibers.

Figure 21 graphs the Izod impact strength measured for the second set of composites. The results from this test are very similar to the initial set. It can clearly be determined that the addition of fibers results in a decrease in Izod impact strength. However, a comparison between fibers or polyamides cannot be made due to the amount of variation and similarity of values.
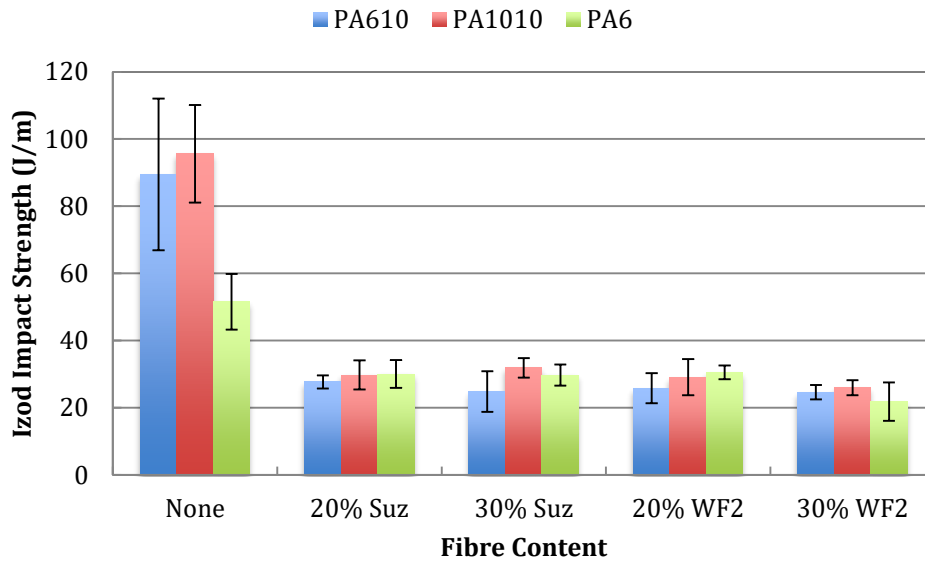
Figure 21 -20% and 30% Fiber content Izod Impact Strength

6.0 Cellulose Compounding with a Polyamide Blend

6.1 Introduction

Based on the results and thermal stability findings on the previous chapter, it is determined that the Suzano fiber would be the most promising filler due to its higher thermal stability. However, the current processing method for Suzano fiber does not result in an easily compoundable product. At a lab scale, it is feasible to grind up the pulp sheet resulting in loose fibers. The texture of these loose fibers does not feed easily into an extruder. Therefore, in order to continue the experimentation process, CreaFill cellulose is used as an alternative substitute for Suzano fiber. CreaFill comes in powder form and can be more easily fed into an extruder.

In comparing the polyamides, there are advantages associated with each. Polyamide 10,10 and 6,10 are 100% and 62% biobased, respectively. Although the cost is higher, the sustainable nature of the material has long term benefits. By investing in bio-based materials now, the technology and cost will develop enough to eventually compete with petroleum based polyamide. Additionally, there is indication in Figure 21 that the impact strength of PA 6,10 and PA 10,10 is higher than recycled PA 6. However, RPA 6 is lower cost than biobased materials. Because it is recycled, the composites produced creates a demand for material that would otherwise go to a landfill. RPA 6 also showed a higher flexural strength than the biobased polyamides. In this next section, a blend of PA 6,10 and RPA 6 will be tested in order to form a hybrid of the aforementioned properties. PA 6,10 is selected because it is more likely to be miscible with PA 6, as discussed previously.

6.2 Results and Discussion

6.2.1 SEM Images

Figure 22 and Figure 23 show a close up SEM image of the fractured surface of a PA 6,10 and RPA 6 composite, respectfully. Both images are at 800x magnification. The PA 6,10 surface can be described as courser than the RPA 6 surface as it has a lot more edges and texture. The RPA 6 surface is smoother but has a lot of light spheres in a variety of sizes. These spheres are attributed to the presence of polypropylene, which is a common contamination in recycled nylon. The most notable difference in the microscopy of these two polyamides is the presence of small amounts of polypropylene in RPA 6, it is immiscible with polyamides and thus forms the smaller cluster of the separate phase. There is also a presence of voids in the recycled PA 6. These are indicated by the black circles. This is important to note that they may be present before any addition of natural fiber. These voids in the image of RPA 6 are attributed to the removal of the polypropylene spheres from the surface at the moment of the fracture.
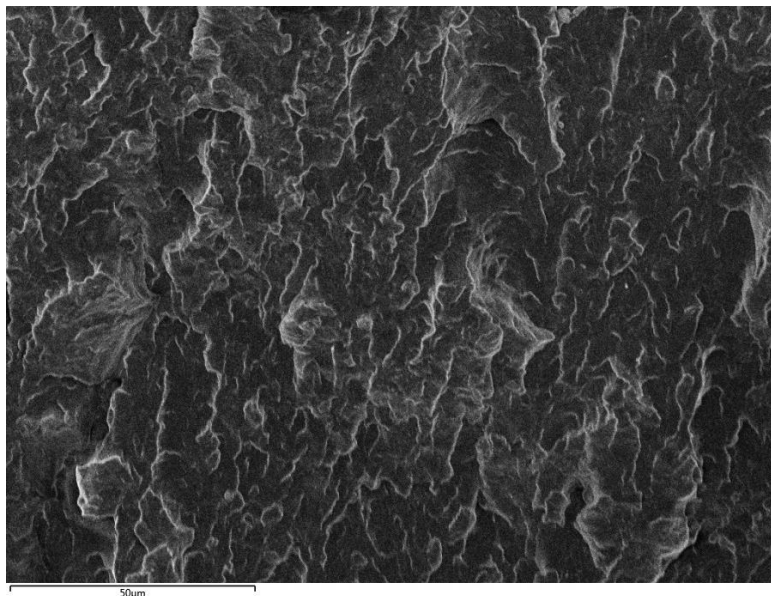
Figure 22 - SEM of PA 610 with x800 magnification
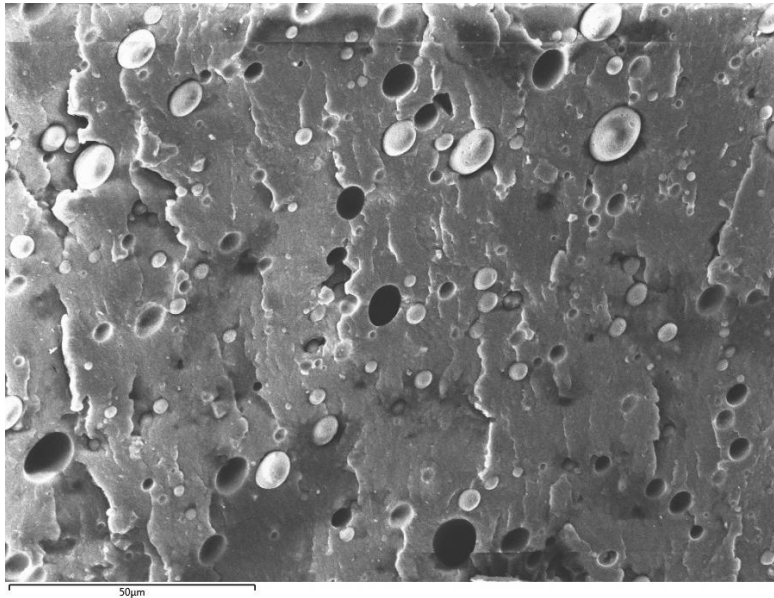
Figure 23 – SEM of RPA 6 with x800 magnification

Figure 23 was used to estimate the amount of polypropylene present based on the ratio of surface area. Appendix D has additional information with regards to the image analysis. The estimated volume fraction of polypropylene shown is 6.2%. Densities of each polymer are used to adjust this ratio into a mass basis of 5.1 wt.-%.

Figure 24 shows the fracture surface of the 30% PA 6,10 and 70% RPA 6 blend. Similar to Figure 23, there are immiscible sections of polypropylene and some voids. However, both visually appear smaller that in RPA 6. The coarseness of the surface is an intermediate between that observed in Figure 22 and Figure 23.
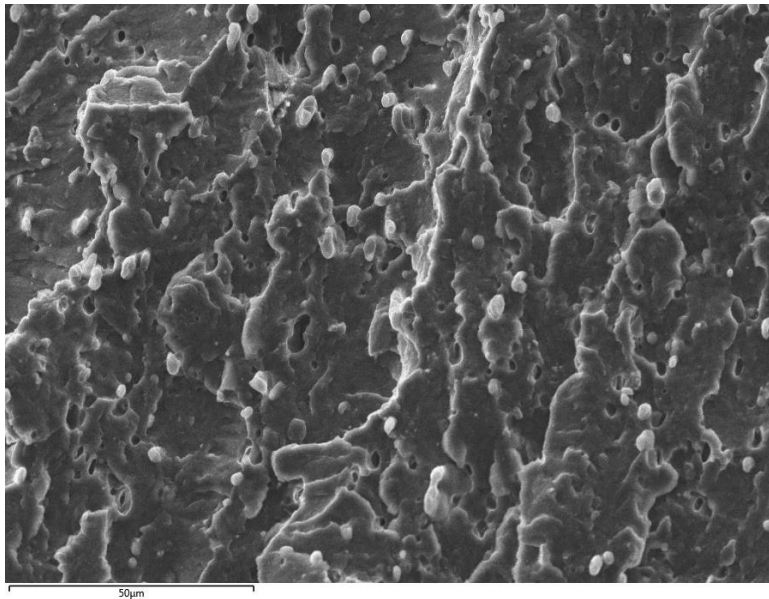
Figure 24 – SEM of PA Blend with x800 magnification

It is important to note that there is no apparent separation of phases between the PA 6,10 and RPA 6. This is a good indication that there was good miscibility of the two polyamides. Without this characteristic, there would be separate phases requiring stress transfer to occur across interfaces. Depending on the nature of that interface, this could potentially result in inferior mechanical properties [57].

The addition of cellulose to the polyamide blend is shown in Figure 25. This image is fairly similar to Figure 24 but with the addition of some smoother patches.
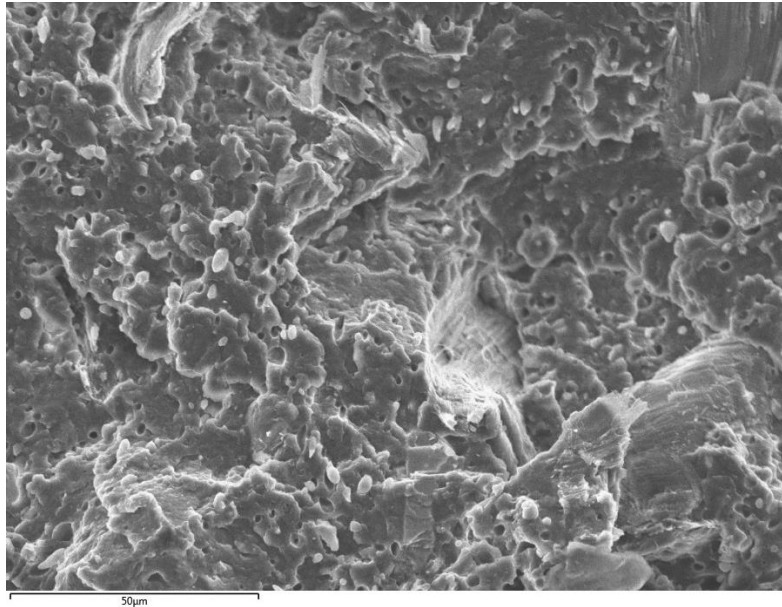
Figure 25 - SEM of 20% Cellulose with x800 magnification

The presence of cellulose is known to increase the brittleness of a composite [43]. Because of this, an impact would have less energy dissipation throughout the composite [58]. Thus, it is possible that the smoother sections observed in Figure 25 are due to more localized fractures from lack of energy dissipation. It is possible that such localization of the fracture could be triggered by concentration of fibers not well dispersed.

Additionally, the presence of cellulose would act as a nucleation point for the crystallization of polyamide. This alters the morphology of the resulting crystalline structure because it is unable to grow in three directions due to one direction being the cellulose fiber. Instead, crystallization occurs normal to the surface, which creates a morphology referred to as transcrystallization [4]. This change would also affect the transfer of energy and result in the different fracture surface.

Another important characteristic of Fig 25, is the absence of any loose fibers. This indicates that fiber pull out is not an issue for this composite. This is expected because

cellulose is reported to have good interfacial adhesion in polyamide due to some similarities in chemical structure [34, 59, 60]. The efficient bonding between the fiber and matrix allows for better stress transfer and thus higher mechanical properties [34].

6.2.2 Mechanical Properties

The tensile properties of the composites are reported in Figure 26 and Figure 27, below. The Young's modulus is observed to generally increase with the addition of cellulose content, with the exception of the 10 percent cellulose composite. This is expected as the cellulose fibers increase the rigidity of the composites. This behaviour is also reported by Amintowlieh [4] and Ozen et al. [42] for other types of fiber in PA6 and by Kiziltas [21], Sears [41], and Xu [34] for cellulose in various polyamides. The PA blend shows intermediate properties between the neat polymers in nearly a proportional amount to the ratio of each polymer added.
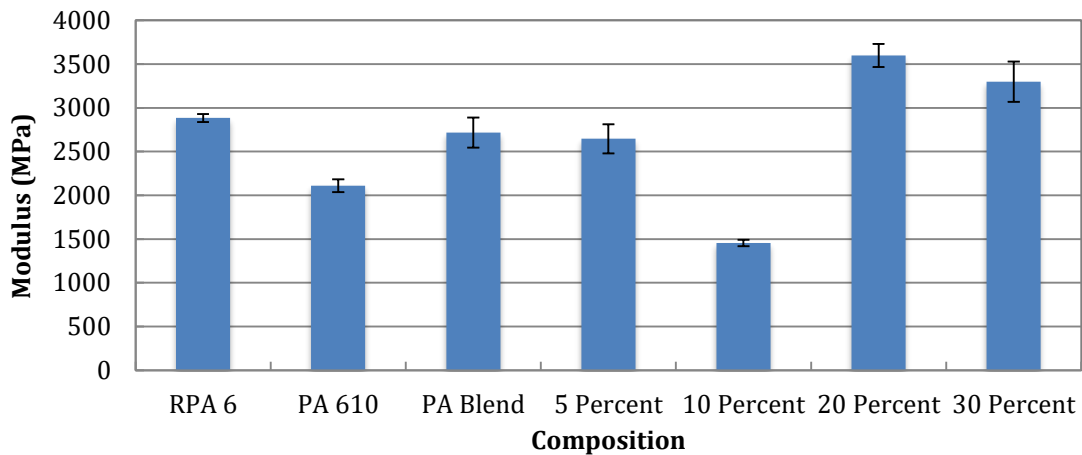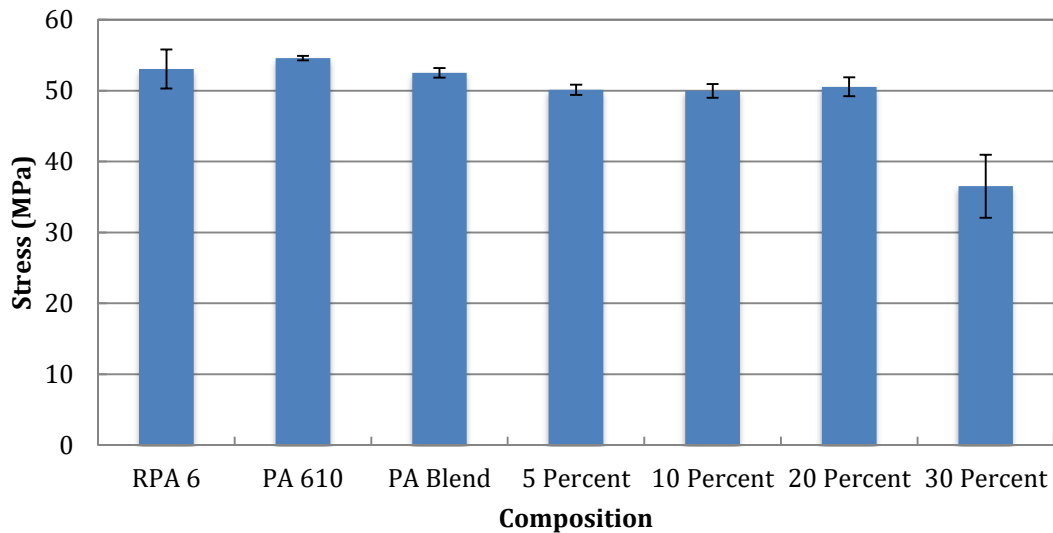
Figure 27 – Tensile Stress at Maximum Load of Cellulose Filled PA Blends

The tensile strength, shown in Figure 27, indicates a decrease in tensile strength with the addition of cellulose fibers. This is unexpected as tensile properties are generally expected to increase with the addition of fiber content [61]. However, at 30% loading dispersion of the fiber becomes more difficult and so this could be an effect of poor distribution. At lower filler amounts, the tensile strength remains approximately the same. The drop in tensile strength above 20% has also been reported in literature [43]. This is due to the increased filler loading starting to interfere with the stress-transfer abilities of the matrix.

The remarkably low Young's modulus value for the 10 percent composite in Figure 26 indicates that there might have been an issue with the compounding of this set. Although caution was taken to maintain consistent experimental parameters for all sets, there are many possible errors that could occur. For example, it is possible that the raw materials were not properly dried due to the sharing of laboratory space. Another possibility is that the manual dial of the extruder speed could have been inconsistently

lower than other days, allowing for more thermal degradation. Although the source of error is unknown, the inconsistent data for the 10 percent composite set indicates that it should be disregarded.

Figure 28 and Figure 29 show the flexural properties for the composites tested. The flexural modulus consistently increases with fiber loading and, similarly to the tensile modulus, the PA Blend has a value in between that of its neat components. The stress at 5% strain also increased by filler content and the 30% cellulose sample would break before this point was reached. These results are also in accordance with literature [43, 21]. Similar to tensile strength, the decrease in flexural strength above 20% can be attributed to the filler loading influencing stress transfer properties [43, 62]. For both flexural properties, the blend tended to have values closer to that of the PA 6,10 even though 70% of the sample consists of RPA 6.
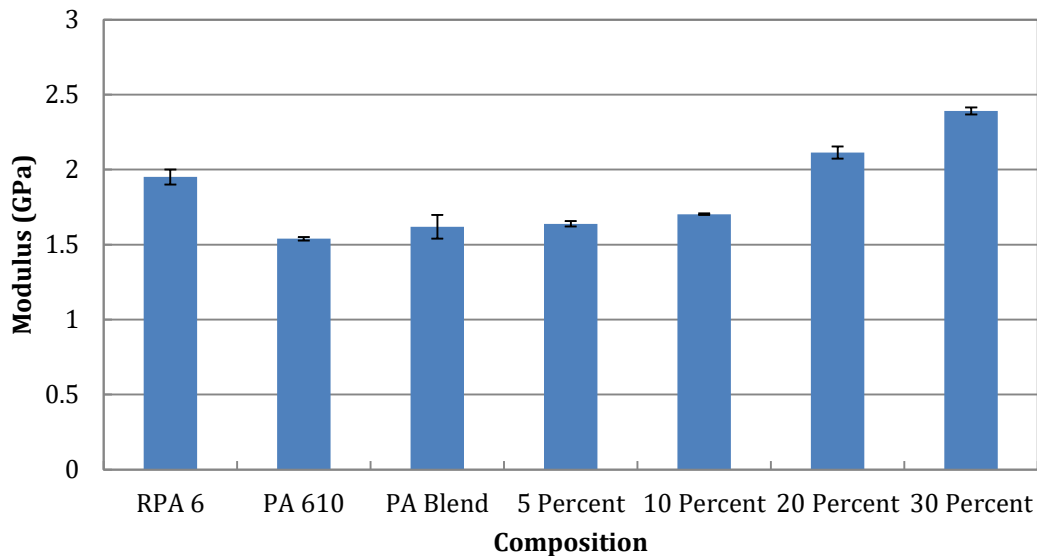
Figure 28 - Flexural Modulus of Cellulose Filled PA Blends
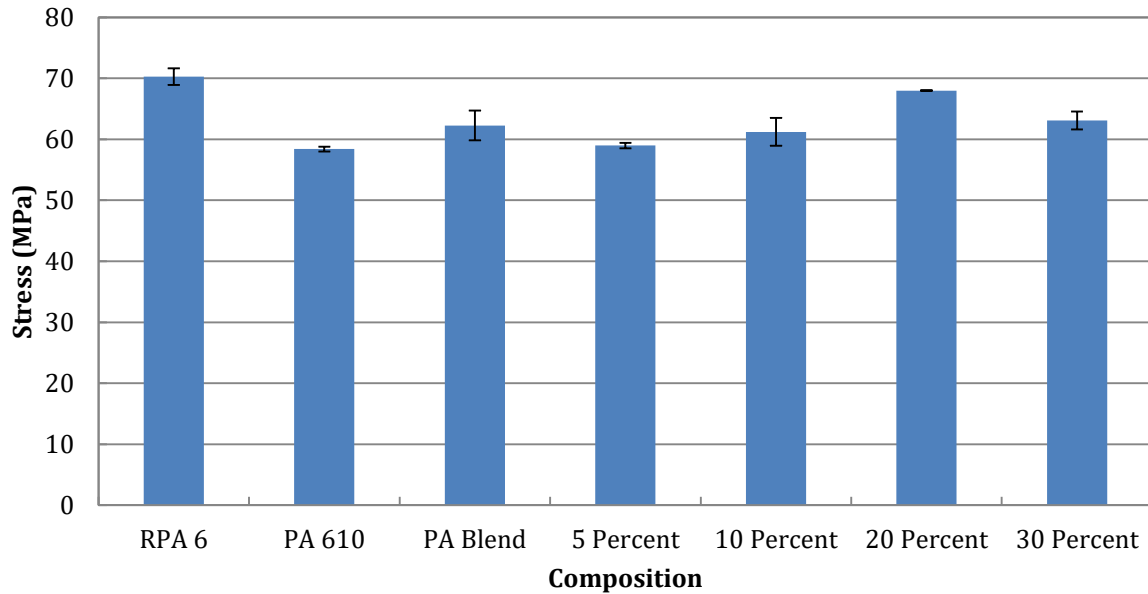
Figure 29 - Stress at 5% Strain of Cellulose Filled PA Blends

Figure 30, below, shows the notched Izod impact strength. The impact strength is shown to decrease with increased fiber content. However, significant reduction does not occur until 30% cellulose content. The increased fiber content reduces the impact strength because the fibers increase the interfacial regions, thereby assisting crack propagation [42, 43]. The blend of polyamides may have slightly reduced impact strength in comparison to the RPA 6, but is generally comparable for the accuracy of the test. The higher value of impact strength in the PA 610 does not appear to increase the impact properties of the blend. However, because the blended polyamide is not significantly lower, it can be assumed that there is no increase in interfacial regions.
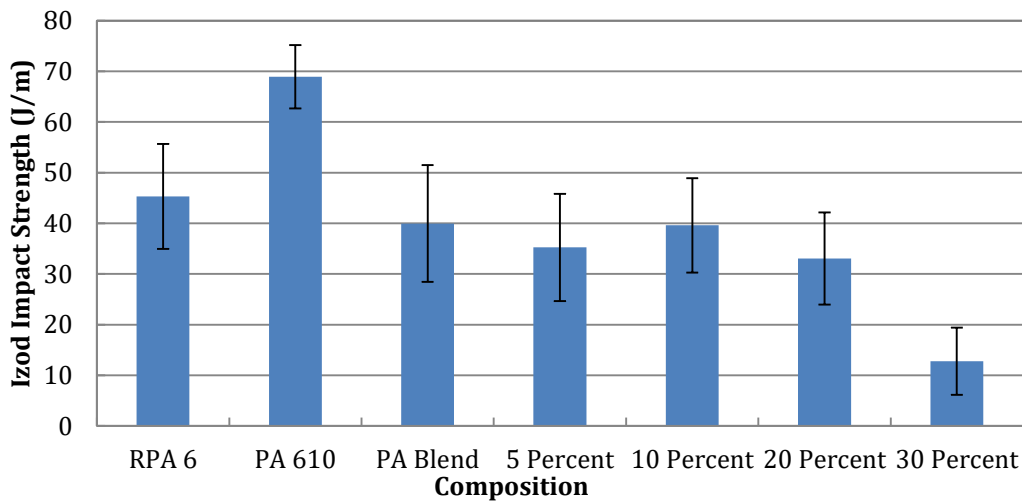
Figure 30 - Notched Izod Impact Strength of Cellulose Filled PA Blends

Although a general increase in properties is observed with the addition of cellulose fiber, the purpose of the composite is to replace the use of glass fiber composites. Therefore, the true performance should be compared to property values of glass fiber composites. However, because of the unique polyamide blend used, there is no available data for comparison. Instead, a comparison of the relative changes in properties due to filler level can be made, as listed in Table 7.

Table 7: Relative Increase of Properties with 20% Filler vs. Neat Polyamide [4]

	20% Cellulose in PA Blend	*20% Glass Fiber in PA 6*
Tensile Strength	-4%	60%
Tensile Modulus	33%	78%
Flexural Strength	9%	68%
Izod Impact Strength	-18%	-10%

The comparison made in Table 7 indicates that the cellulose composites do not increase the property values as much as glass fiber. However, the use of cellulose instead of glass fiber can still be an advantage due to the lighter density and processing advantages. The application of these composites would depend on the required mechanical property specifications of a component.

6.2.3 Thermal Properties

Figure 31 and Figure 32 show the power-temperature DSC curves of the composite samples, separated by first cooling curves and second heating curves, respectively. The sharpest and clearest curve is that of pure PA 610. RPA 6 also has a narrow peak but also has a second, smaller peak, which is attributed to the small amounts of polypropylene present. As cellulose content is added, the curves become broader and less sharp.
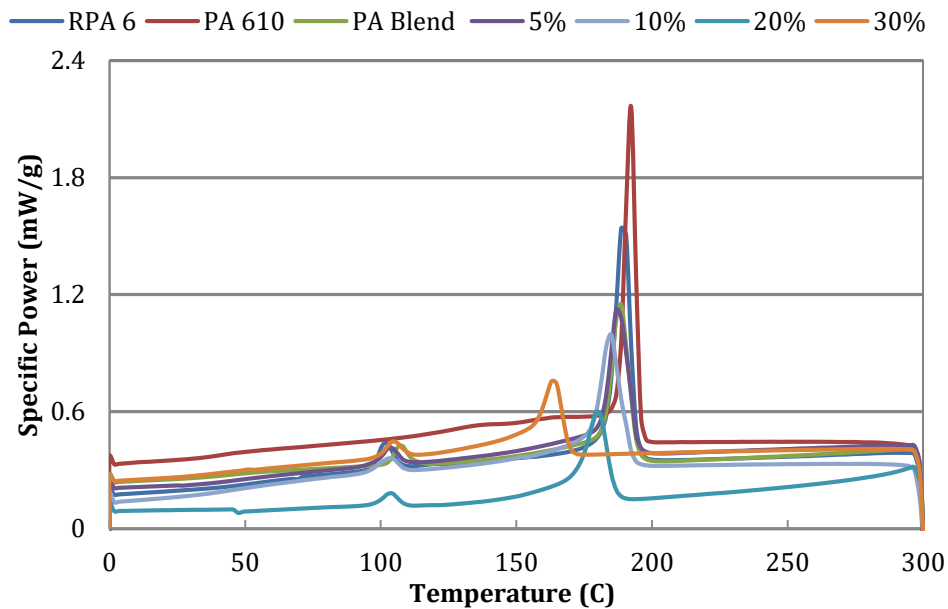
Figure 31 – DSC Cooling Curves
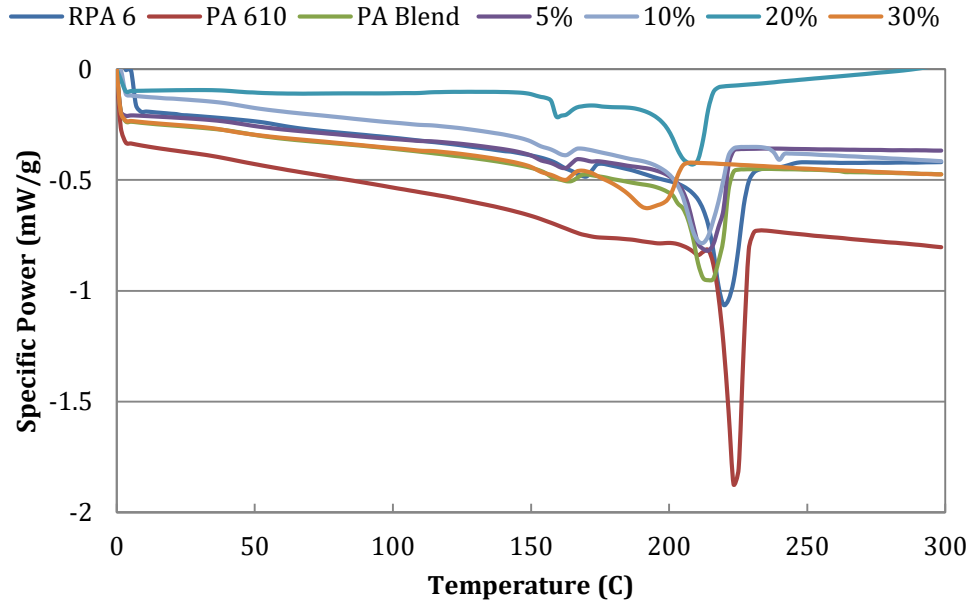
Figure 32 – DSC Second Heating Curves

From these DSC curves, the melting and crystallization enthalpy can be determined by integrating the area underneath each peak. Table 8 lists the resulting enthalpies calculated for each peak. The major peaks are associated with the crystallization of polyamide while the minor peaks are due to the existing polypropylene.

Table 8: Melt and Crystallization Enthalpies

	Melt Enthalpy (J/g)		Crystallization Enthalpy (J/g)	
	Major Peak	Minor Peak	Major Peak	Minor Peak
PA 6	94.99	4.56	88.42	5.38
PA 610	113.13	0.00	127.94	0.00
PA Blend	87.99	3.58	77.14	4.06
5%	93.86	3.86	74.20	4.65
10%	76.18	3.25	80.44	4.07
20%	48.07	3.74	44.39	2.45
30%	45.95	3.41	45.89	3.13

From the above enthalpies, the crystallinity within each phase can be calculated, as described in the Experimental Section. Figure 33 and Figure 34, below, graph the resulting values obtained from both the measured melt enthalpy and the crystallization enthalpy.
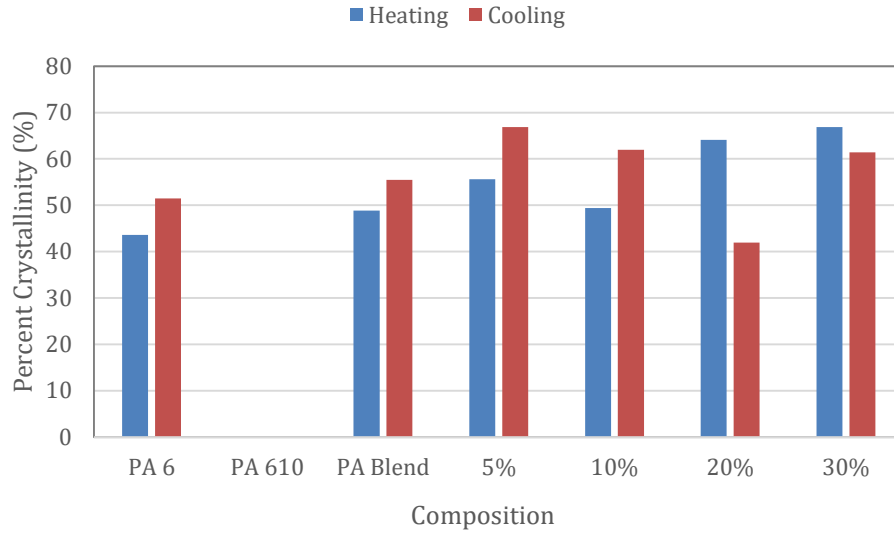
Figure 33 – Polypropylene Percent Crystallinity

The fraction of crystallinity in the polypropylene phase is not expected to change significantly between composites due to the characteristics being altered occurring in the polyamide phase. Figure 33 shows that the observed PP crystallinity ranges from 40-70%. This range encompasses the generally reported value for polypropylene degree of crystallinity, which is 55-60% [63]. This wide range of values is because there is only a small amount of PP present. The error associated with calculating the enthalpy under the curve is greater for polypropylene because the small size of the peak allows for significant change in area as the fitted line is adjusted.
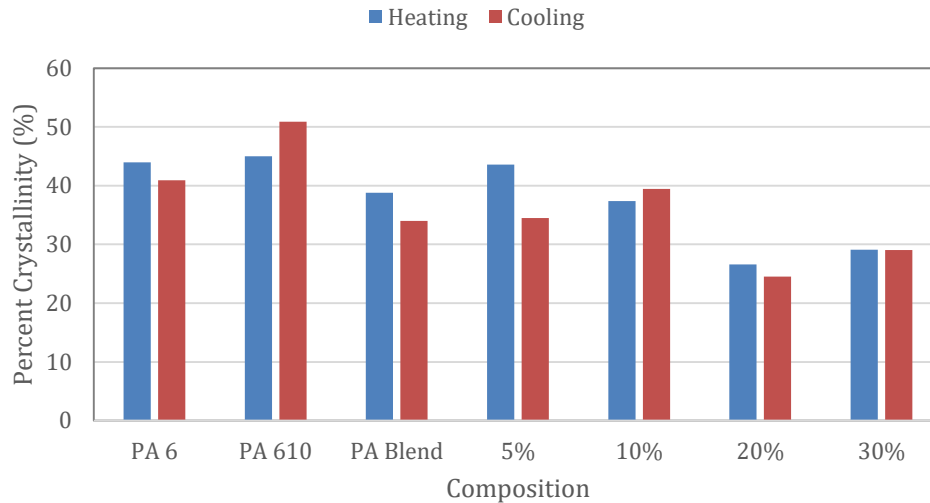
Figure 34 – Polyamide Crystallinity

Figure 34 demonstrates slightly less variation in the calculation of crystallinity. Generally, the values calculated with the melt enthalpy are comparable to those calculated with the crystallization enthalpy. In comparison to the PA blend, the 5% and 10% composites show either a slight increase in degree of crystallinity or remain approximately the same. However, the higher value cellulose composites appear to reduce the amount of crystallization to occur in the polyamide phase. The introduction of cellulose fiber into the polyamide matrix has two contrasting effects on the crystallinity. One effect of the presence of cellulose fibers within the matrix would be to hinder the movement of the polyamide chains. This would reduce the ability of the chains to fold into crystalline structures and interfere with the growth of crystallites. Figure 34 indicates that this effect has a stronger influence on crystallinity at the higher cellulose levels of 20 and 30 percent. At the lower filler levels of 5% and 10% cellulose, this affect does not appear to lower the crystallinity. Similar observation has been reported by Kiziltas et al. [64, 44].

Although limiting the growth of crystallites, the presence of cellulose is expected to act as a nucleating point for crystallization to occur. However, this would also result in an increase in crystallization temperature [65]. Table 9 indicates that this is not the case.

Table 9: Crystallization and Melt Temperatures

	Crystallization Temperature (°C)	Melting Temperature (°C)
RPA 6	190.1	214.1
PA 610	193.0	223.3
PA Blend	188.6	214.6
5 Percent	187.7	214.2
10 Percent	177.7	204.8
20 Percent	180.5	208.8
30 Percent	164.8	191.8

In Table 7, there is an observed decrease in crystallization and melt temperature as the filler level of cellulose is increased, most significantly from 20% to 30%. This is opposite to what is expected with increased nucleation. A similar study by Amintowlieh demonstrates the expected increase in crystallization temperature with the addition of wheat straw as a reinforcing fiber. Other studies by Kiziltas et al. report no change to the melt and crystallization temperatures with the use of microcrystalline cellulose [43, 64]. However, a similar decrease in melt temperature has been reported by Dweiri and Azhari in the study of sugarcane bagasse fiber in polyamide 6 [66]. It is suggested that the lower temperatures could be due to changes in the type and size of crystal structure formed. As more nucleating sites are available, the amount of growth available before interfering with another crystal is reduced. Additionally, it is proposed that depression of melt temperature could indicate partial miscibility of the cellulose fibers in the amorphous sections of the polyamide matrix and strong molecular interactions [66]. This depression of melt point has been utilized in the study of polymer segment interactions [67]. The effect of this decrease in melt temperature is larger when there are strong intermolecular interactions, such as hydrogen bonding [68]. This is the case for cellulose in polyamide as the strong interaction is what allows for good adhesion and mechanical stress transfer. It is also suggested that once cellulose is added, there is possibility of diffusion of low molecular weight substances from the fiber to the matrix. This would have similar effect to plasticizer, which would lower the melting temperature [4].

For the purpose of under-the-hood applications, the decrease in melt temperature is undesirable. However, the amount of decrease is not significant until 30% cellulose content is used. At 20% cellulose, there is less than a 6°C decrease from the melting temperature of the polyamide blend.

Figure 35 plots the thermal gravimetric analysis curve for each composite at a heating rate of 10°C/min. These curves show the expected decrease in onset temperature as cellulose content is added. The 20% and 30% composites have much broader slopes than the lower cellulose content composites.
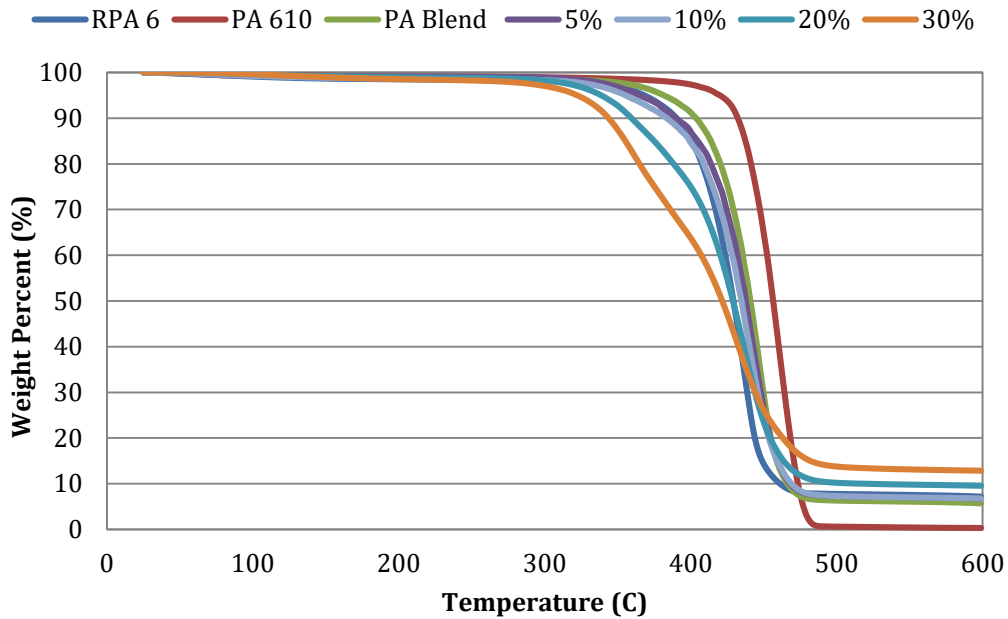
Figure 35 – TGA curves of neat polymers and composites

Although the cellulose-filled composites still show higher thermal degradation, the temperatures at which these become relevant are much higher than expected process temperatures. Figure 36 graphs the 2 percent weight loss temperatures of the composites.
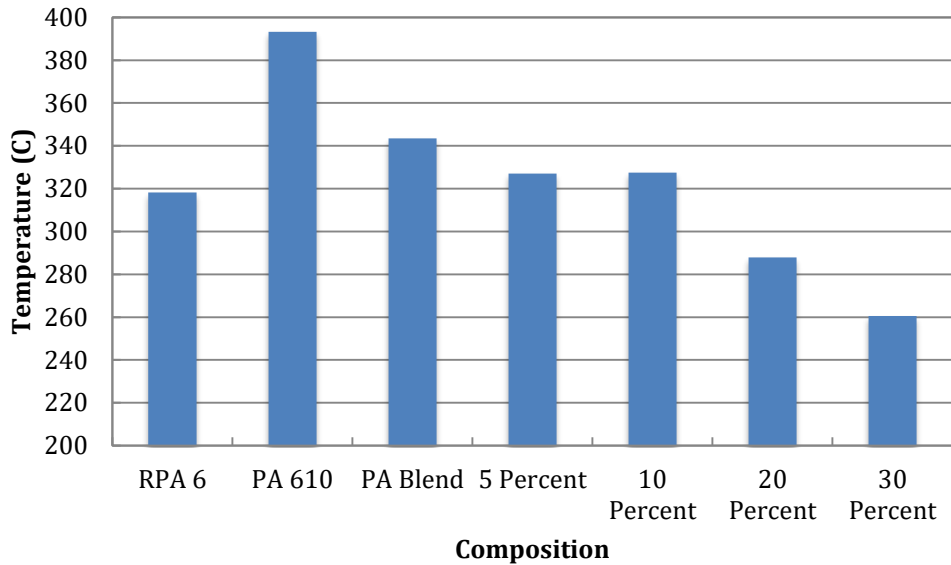
Figure 36 - Temperature of 2% Weight Loss of Cellulose Filled PA Blends

It can be observed that increasing cellulose content slightly reduces the temperature at which 2 percent weight is lost. This is known to occur because the cellulose fiber remains less thermally stable than polyamide. The PA blend provides increased thermal stability. This increase makes the 5% cellulose composite comparable to the RPA 6. However, all temperatures are well above process conditions. Even at the 30% cellulose level, 98% of the composite weight is retained until over 260 °C.

Figure 37 graphs the weight percent that remains after the composites are held at 600 °C for 5 minutes. It can be observed that the presence of cellulose significantly increases the amount of remaining ash content.
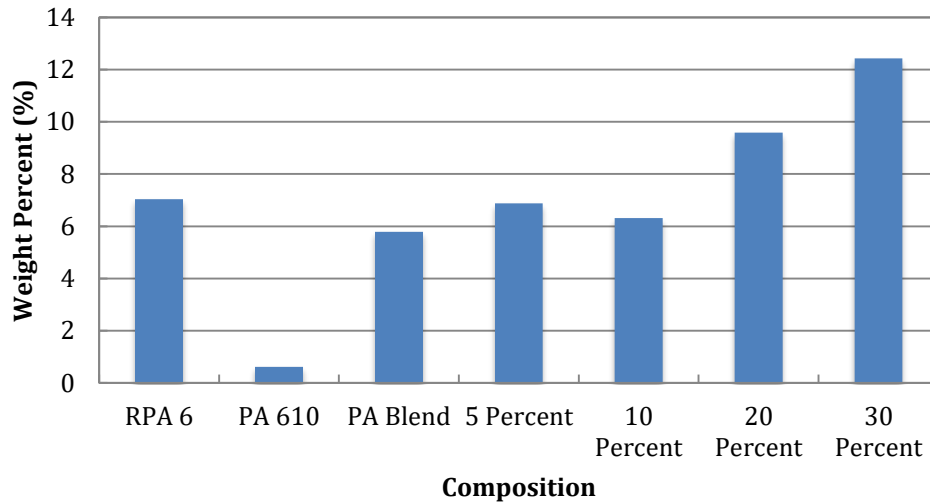
Figure 37 - TGA Ash Content at 600˚C of Cellulose Filled PA Blends

The remaining ash content is the result of thermal degradation solid byproducts. The thermal degradation of PA 610 leaves relatively no solid product, while the increase of cellulose content increases the solid residue. This is beneficial to the composite because ash content increases the flame retardancy of a material. This is because the residual ash content can act as a physical barrier to the rest of a composite which can slow down heat flow and thus delay the burning process [69].

6.3 Odor Additive - RP 17

The use of RP17 as an additive is designed to eliminate the strong smell of the composite that can be caused by the thermal degradation of the fibers. The use of the additive is mainly to mitigate any possible unpleasant odor of a composite part. The use is not intended to have any effect on the mechanical properties. The ability of the additive to improve the smell is not included in the scope of this thesis. However, a comparison of composites with and without the additive is conducted to ensure that the mechanical properties are not negatively affected by its use. The comparison is conducted at the 20% cellulose level.

Figure 38, below, shows a comparison of the flexural modulus. In comparison with the polyamide blend, it can be seen that the values are very similar. However, an analysis of variance concludes that the difference in values is statistically significant. The ANOVA table for this can be found in Appendix B.
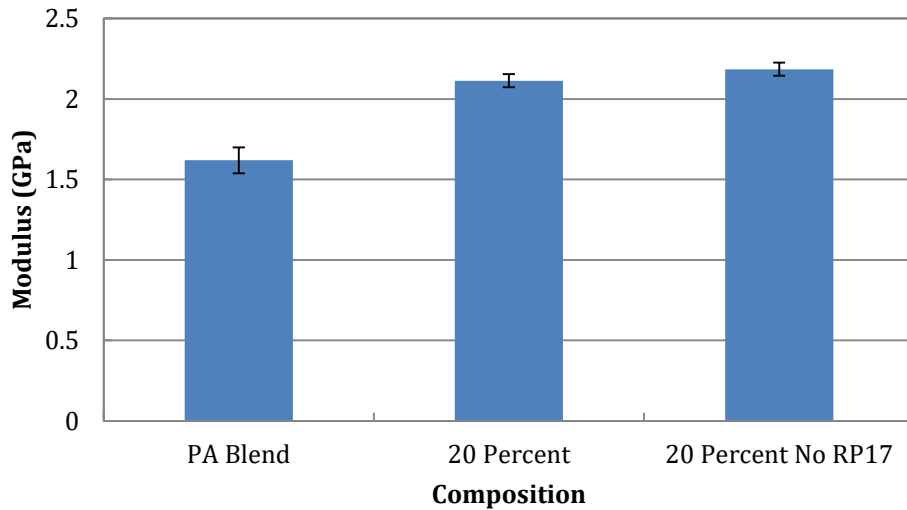
Figure 38 - Flexural Modulus Comparison of RP17

Although the additive has been shown to reduce the value of the flexural modulus, the amount of change is very slight, The addition of RP17 increases the flexural modulus by only 3 percent as shown in Figure 38.

Contrarily to the flexural modulus, the additive appears to increase the stress at 5% strain, as shown below, in Figure 39.
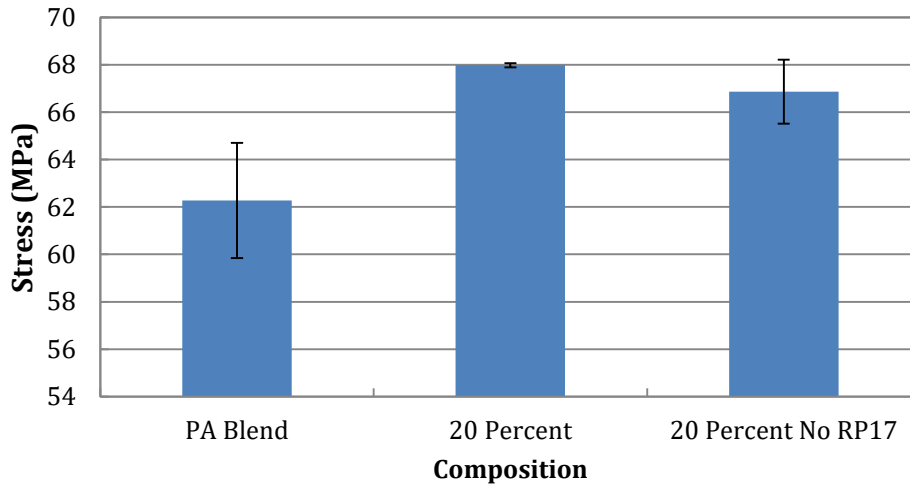
Figure 39 - Stress at 5% Strain Comparison of RP17

However, the ANOVA table, in Appendix B, indicates that the difference is not statistically significant. Therefore, it can be concluded that RP17 does not affect the stress at 5% strain.

Figure 40 and Figure 41 compare the tensile modulus and stress properties. Both properties are found to have statistically significant differences in values.
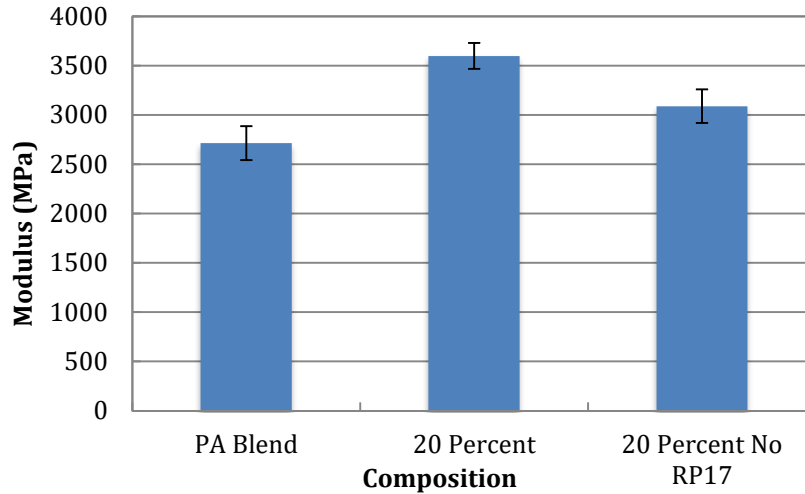
Figure 40 – Young's Modulus Comparison of RP17
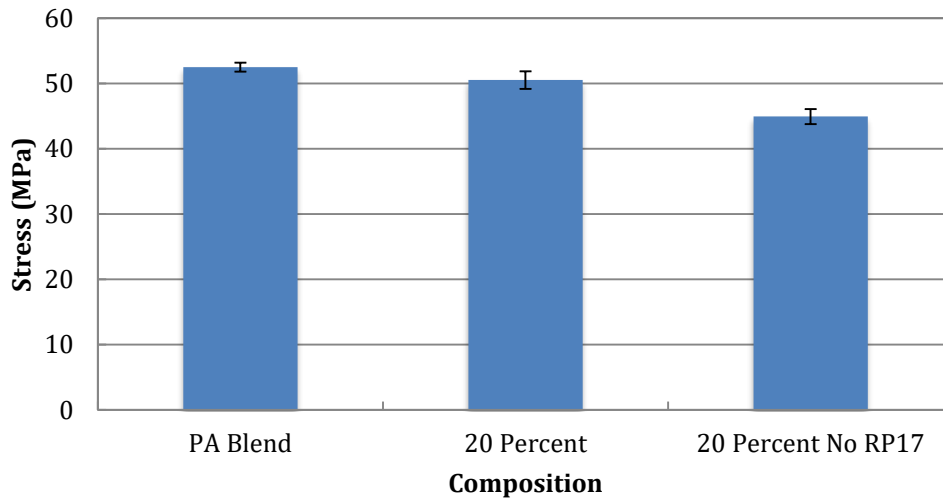
Figure 41 - Tensile Stress at Maximum Load Comparison of RP17

The Young's modulus and tensile stress are shown to increase with the addition of the RP17 additive. The increases are 16% and 12%, respectively. Figure 42, below, shows the measured Izod impact strength for the composites with and without the additive.
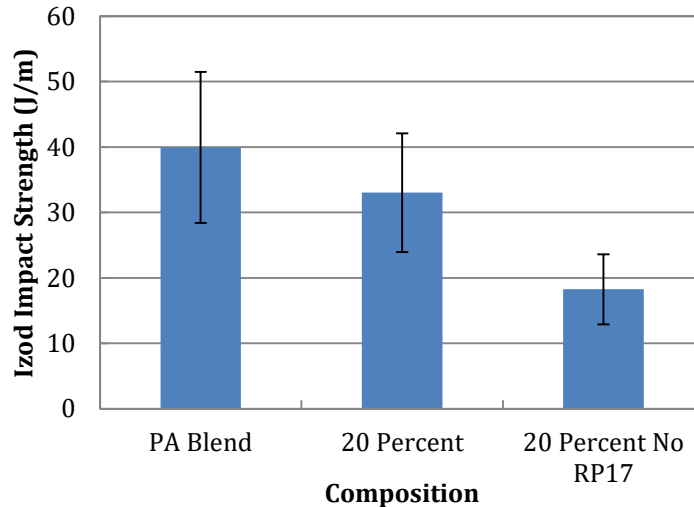
Figure 42 – Izod Impact Strength Comparison of RP17

In this figure, it can be seen that the composite with RP17 has higher impact strength. The ANOVA table, recorded in Appendix B, concludes that the difference is significant, despite the high variation in data. The composite with the additive is 80% higher than without.

Although the addition of 1% RP17 was not expected to affect the mechanical property values, it has been determined that some of the properties are influenced. However, most of these affects improve the composite properties. The Young's modulus, tensile stress, and Izod impact strength are all benefited by the use of the additive. The only observed detriment to property is in the flexural modulus, which is very slight. Overall, the use of RP17 would seem to improve the resulting composite. However, these composites have no other additives in consideration. It is possible that these same improvements could be achieved through another additive at a lower cost. The usefulness of RP17 can only be determined through odor tests, because that is its purpose. However, for the purpose of this research, it can be concluded that its used does not negatively affect results.

6.4 Carbon Fiber

Carbon fiber is known to be a highly effective reinforcing filler but the high cost prevents it feasibility for many applications. However, market forecasts compare the history of carbon fiber to that of fiberglass [50]. The trend indicates that costs may reduce enough to make carbon fiber a viable option in the future. Because of this, carbon fiber is also considered in this research as an option to create a hybrid product containing both cellulose and carbon fiber. In this investigation, hybrid composites are produced containing both cellulose and carbon fiber. The 20% and 30% filler levels are investigated by replacing part of the cellulose with carbon fiber to get a composite with 10% cellulose and 10% carbon fiber, referred to as the 10%/10% mixture and another composite with 10% cellulose and 20% carbon fiber, referred to as the 10%/20% mixture.

The data obtained from the carbon fiber composites can be interpreted in two ways. The first perspective considers a filler level and compares the differences between that filler being all cellulose or a combination of cellulose and carbon fiber. For example, at the 20% filler level, a comparison of 20% cellulose versus 10%/10% mixture can be made. The second option is to observe just the effects of adding more carbon fiber by only looking at varying levels of carbon fiber content. In this case, the composites of interest would include 10% cellulose, 10%/10% mixture, and 10%/20% mixture.

Figure 43 shows the flexural modulus of the aforementioned composites. In comparing the 20% cellulose to the 10%/10% mixture, the values are very similar, showing no change to the modulus. At the 30% filler content, an increase is shown with the use of carbon fiber.
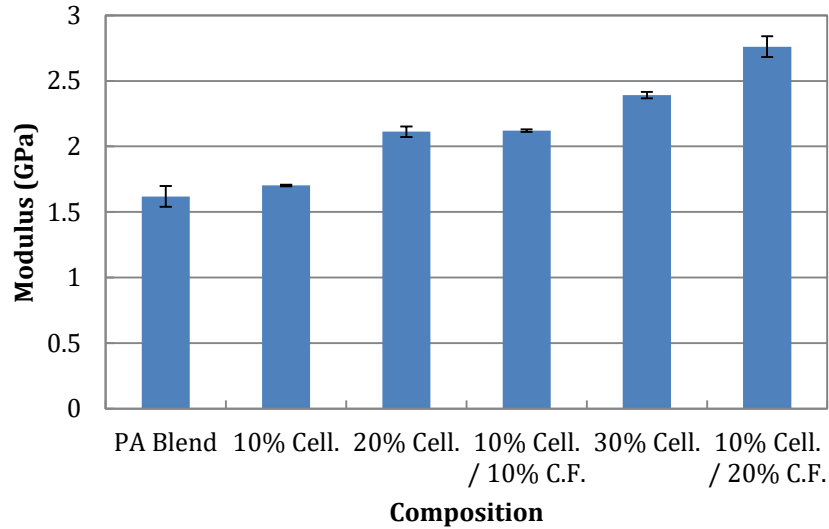
Figure 43 - Flexural Modulus of Carbon Fiber Composites

Similarly, Figure 44 shows the 20% filler level nearly the same, although there is a slight decrease, while at 30%, carbon fiber significantly increases the stress at 5% strain.
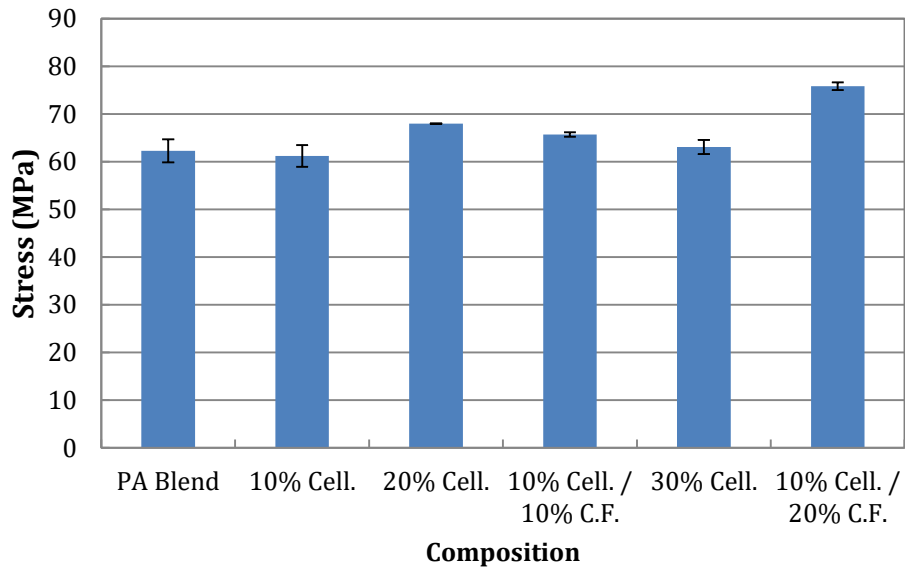
Figure 44 - Stress at 5% Strain of Carbon Fiber Composites

In contrast to the last two figures, there is a significant drop in Young's modulus for carbon fiber at the 20 percent filler level, as shown in Figure 45. The Young's modulus is

50% lower for the mixture of carbon fiber and cellulose, as opposed to the pure cellulose. However, this significant decrease is not observed at the 30% filler level.
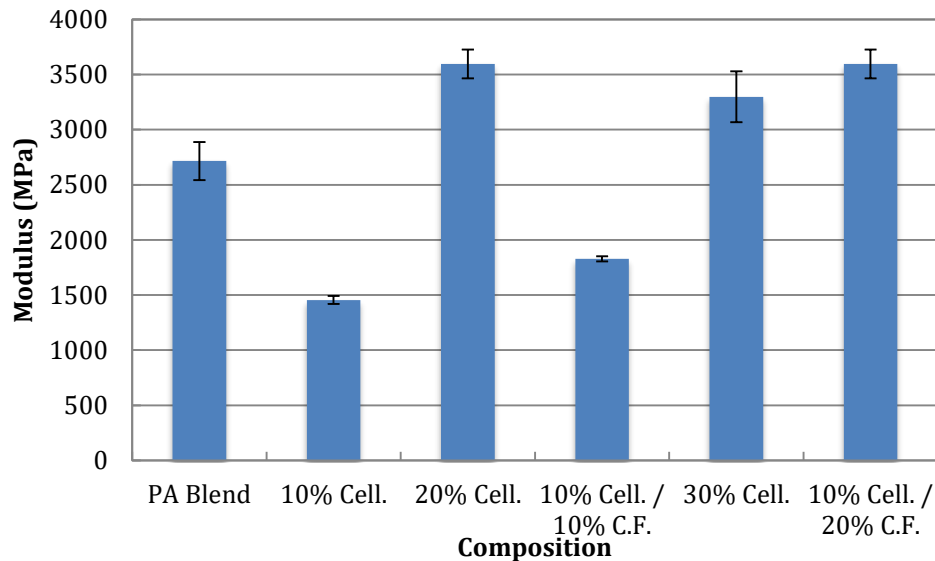
Figure 45 - Young's Modulus of Carbon Fiber Composites

This unexpected trend can be explained by considering the carbon fiber level only. In comparison to the 10% cellulose, which can be considered the 0% carbon fiber level, the 10% and 20% carbon fiber levels do still show a consistent increase. There has already been discussion of the 10% cellulose composite having unusually low values. It has been suggested that there was an error during compounding that negatively affected the mechanical properties. The same 10% cellulose compound was then used to create the two levels of carbon fiber composites. Therefore, it follows that these composites would still have the same issue that the 10% cellulose composite demonstrates. Limited amount of carbon fiber did not allow for replication. Due to this problem, the comparison at specific filler levels cannot be used to directly compare cellulose to carbon fiber. With this in consideration, the comparisons must account for the initial 10% cellulose property values.

Figure 46, below, shows the tensile stress measured for the composites. However, other than the 30% cellulose composite, the values reported are all very similar to the PA blend.
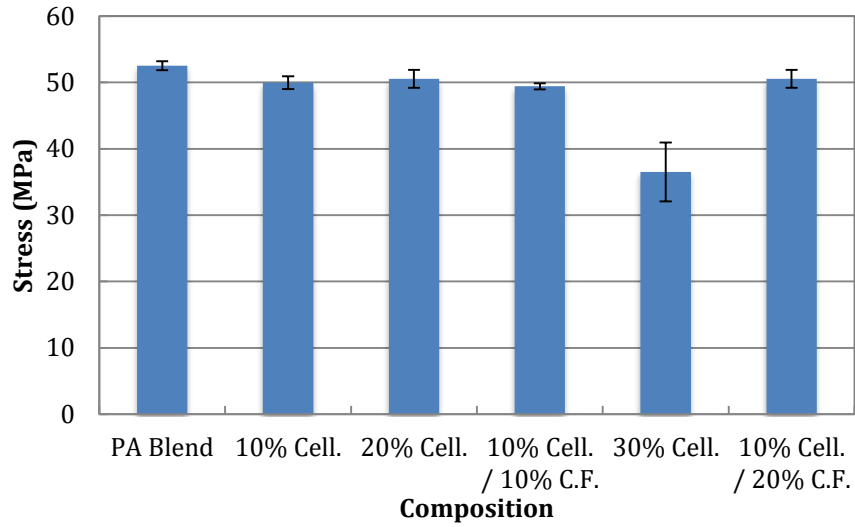
Figure 46 - Tensile Stress at Maximum Load of Carbon Fiber Composites

This would imply that neither fiber has a significant effect on the tensile stress at maximum load, with the exception of the 30% cellulose. Looking only at carbon fiber level, there is no significant change in value between levels.

The Izod impact strength is reported in Figure 47. The addition of carbon fiber to the 10% cellulose composite does not appear to further reduce the impact strength. While there is a significant decrease from 20% cellulose to 30% cellulose, there is no change between the 10% and 20% carbon fiber levels.
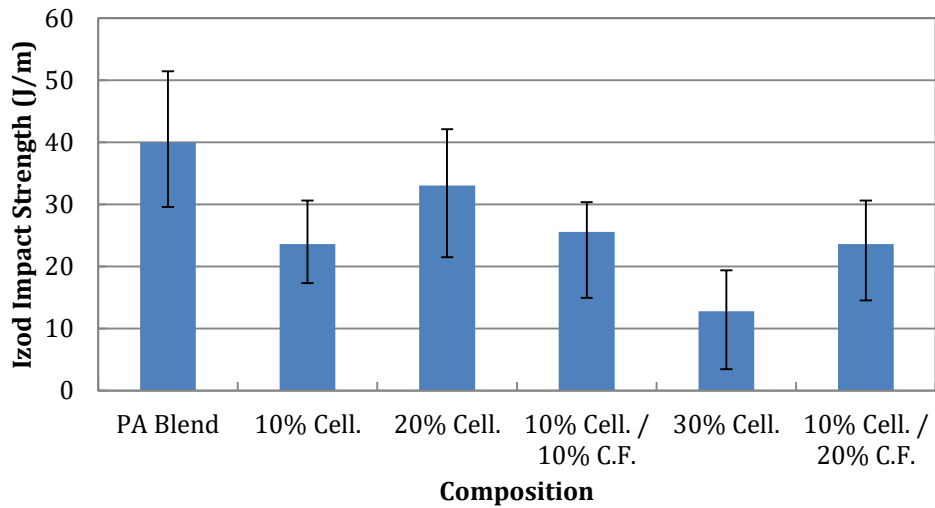
Figure 47 - Izod Impact Strength of Carbon Fiber Composites

This result is the most interesting because it is unlike the trend observed for pure cellulose. With only cellulose, the filler causes the sample to become more rigid which, although increasing the flexural and tensile properties, results in lower impact strength. However, with the carbon fiber, the same properties still have increase while the impact strength is maintained the same. This indicates that the carbon fiber allows for more impact energy to be distributed by the composite. However, it cannot be confirmed whether the impact strength would be as high as the PA blend, due to the compounding error.

Overall, the effects of increasing carbon fiber are similar to increasing cellulose. Regrettably, cellulose and carbon fiber were not able to be directly compared due to the unusual 10% cellulose data. The main benefit the carbon fiber composites is the consistent impact strength, whereas the cellulose composites show decline with the addition of fibers.

7.0 Conclusions

Through thermal and mechanical comparisons, it was determined that the Suzano fiber had the highest improvement of mechanical properties when compounded with each polyamide. This is due to the higher cellulose content as a result of the fiber's processing method. However, the disadvantage of the Suzano fiber is its ability to feed into the processing equipment.

Further investigation into ultraviolet radiation as a method to increase thermal stability was unsuccessful. Slight increase was observed for the fibers with less cellulose. However, a decrease in thermal stability occurred for the higher cellulose content fiber. Thus, it is concluded that UV treatment is more suitable for fibers with high amounts of lignin.

Overall, the 20% cellulose level resulted in the most favourable combination of properties. Although the 30% level has the highest flexural modulus, there is also abrupt decrease in tensile stress and impact strength between the 20% and 30% filler levels. Furthermore, 20% filler level showed the highest relative increase to the flexural stress at 5% strain and the Young's Modulus. Poorer values at 30% cellulose content are attributed to high filler levels causing fiber agglomeration. This results in ineffective stress transfer within the matrix.

The relative changes in properties for 20% cellulose versus 20% glass fiber was made compared to unfilled polyamide blend and polyamide 6, respectively. The comparison between these relative amounts showed a greater increase in property values for glass fiber. However, the relative increases for the 20% cellulose and its lower density can still prove advantageous for applications that do not require the full capacity of glass fiber composite properties.

The blending of RPA 6 and PA 6,10 generally resulted in intermediate property values. The flexural modulus, melting temperature, and crystallization temperature had

intermediate values that tended toward the lower property value. The addition of PA 6,10 did not significantly improve the mechanical or thermal properties of RPA 6. From the comparison of mechanical and thermal properties, the addition of PA 6,10 tends to be a disadvantage. This is observed in the decrease of tensile modulus, flexural modulus, and flexural stress. Additionally, the melt temperature of PA 6,10 is higher, which requires more energy and would result in more thermal degradation. The use of PA 6,10 is good for sustainability because of its bio-content but must be balanced with the additional cost.

Although the addition of carbon fiber does show relative increase to mechanical properties, the amount of increase is comparable to that of the cellulose filler. Because cellulose fiber is significantly cheaper and easier to process, the application of carbon fiber filler is unnecessary. However, the preserving of impact strength while also improving other mechanical properties is a significant advantage. Particular component specifications would need to be considered in order to determine what levels of impact strength would be acceptable.

8.0 Recommendations

It is shown that a 20% cellulose fiber composite could potentially be suitable for under-the-hood applications. However, these composites have not shown property value increase equivalent to glass fiber. It is recommended that natural fiber composites can be used to replace glass fiber in components that do not require the full extent of fiberglass material properties. Additionally, further testing of durability and other untested properties must be performed in order to evaluate eligibility based on full component specifications.

From the selection of commercially available wood fibers, it was shown that the compounding of the Suzano fiber had the highest increase in material properties. However, the original form of the fiber is difficult for compounding. Therefore, it is recommended that a method of pre-processing the fiber be developed in order to enable easy compounding with the polyamide.

It is recommended that the use of PA 6,10 in a polyamide blend be further analyzed to justify its additional cost. It is concluded that the blending of PA 6,10 in PA 6 generally decreases the desired properties. However, the incentive to use PA 6,10 is that it is partially bio-based and has lower moisture absorption. The effect of moisture absorption on the composites should be further investigated to determine if PA 6,10 could improve the economic viability of its use.

Due to limited resources, the investigation of carbon fiber and cellulose hybrid composites could not be directly compared to the cellulose composites. It is therefore recommended that further investigation be performed when more material is available.

References

[1]   National Highway Traffic Safety Administration, "Summary of Fuel Economy Performance," U.S. Departemetn of Transportation, Washington DC, 2014.

[2]   Nation Highway Traffic Safety Administration, "Federal Register," National Archives and Records Administration, 2012.

[3]   W. J. Joost, "Reducing Vehicle Weight and Improving U.S. Energy Efficiency Using Integrated Computational Materials Engineering," *The Journal of The Minerals, Metals & Materials Society,* vol. 64, no. 9, pp. 1032-1038, 2012.

[4]   Y. Amintowlieh, "Nylon-6/Agricultural Filler Composites," *University of Waterloo,* p. Thesis, 2010.

[5]   American Chemistry Council, "Plastics and Polymer Composites in Light Vehicles," Economics & Statistics Department, 2015.

[6]   A. Abdal-hay, N. P. G. Suardana, D. Y. Jung, K.-S. Choi and J. K. Lim, "Effect of Diameters and Alkali Treatment on the," *International Journal of Precision Engineering and Manufacturing,* vol. 13, no. 7, pp. 1199-1206 , 2012.

[7]   A. Michael and A. Irene, Handbook of Textile Processing Chemicals, Synapse Information Resources, Inc., 2013.

[8]   W. Nelson, Nylon Plastics Technology, London: The Butterworth Group, 1976.

[9]   L. Sperling, Introduction to Physical Polymer Science, 2nd Edition ed., Bethlehem, Pennsylvania: John Wiley & Sons, Inc., 1992.

[10]   Department of Polymer Science, ""Nylon [Pictures Only]"," University of Southern Mississippi, 2005. [Online]. Available: http://pslc.ws/macrog/nylon.htm. [Accessed 23 November 2014].

[11]   S. Dasgupta, W. B. Hammond and W. A. Goddard III, "Crystal Structures and Properties of Nylon Polymers from Theory," *Journal of the American Chemical Society,* vol. 118, no. 49, pp. 12291-12301, 1996.

[12]   B. Majumdar, H. Keskkula and D. R. Pault , "Mechanical behaviour and morphology of toughened aliphatic polyamides," *Polymer,* vol. 35, no. 7, pp. 1399-1408, 16 April 1993.

[13]   B. Majumdar, H. Keskkula and D. R. Paul, "Effectof the nature of the polyamide on the properties and morphology of compatibilized nylon/acrylonitrile-butadiene-styrene blends," *Polymer,* vol. 35, no. 25, pp. 5468-5477, 24 January 1994.

[14]   T. Fornes and D. Paul, "Structure and Properties of NAnocomposites based on Nylon-11 and -12 Compared with Those Based on Nylon-6," *Macromolecules,* vol. 37, no. 20, p. 7698, 2004.

[15]   G. Odian, Principles of Polymerization, Fourth Edition, New York: Wiley Interscience, 2004.

[16]   D. E. Floyd, Polyamide Resins, New York: Reinhold Publishing Corporation, 1966.

[17] L. Hollaway, Handbook of Polymer Composites for Engineers, England: Woodhead Publishing Ltd, 1994.

[18] A. M. Shibley, Handbook of Composites, L. George, Ed., New York: Van Nostrand Reinhold Company Inc., 1982.

[19] W. Chow and Z. Mohd Izak, "Polyamide blend-based nanocompposites: A Review," *eXPRESS Polymer Letters,* vol. 9, no. 3, pp. 211-232, 2015.

[20] J. Chen, W. Wu, C. Chen and S. He, "Toughened Nylon66/Nylon6 Ternary Nanocompositesby Elastomers," *Journal of Applied Polymer Science,* vol. 115, pp. 588-598, 2010.

[21] A. Kiziltas and E. C. Lee, "Sustainable Composites Based on Polyamides and Cellulose Fibers," 2014.

[22] T. S. Ellis, "Miscibillity and Immiscibility of Polyamide Blends," *Macromoleculs,* vol. 22, no. 2, pp. 742-754, 1989.

[23] T. S. Ellis, "Mixing Relationships in Aliphatic Polyamide Blends," *Polymer,* vol. 33, no. 7, pp. 1470-1476, 1992.

[24] Rapra Review Reports, "Polyamides as Engineering Thermoplastic Materials," Rapra Technology Limited, Shropshire, 2000.

[25] T. Q. Hu, Characterization of lignocellulosic materials, Oxford: Blackwell, 2008.

[26] M. Lewin and I. S. Goldstein, Wood Structure and Composition, New York: Marcel Dekker, Inc., 1991.

[27] C. J. Biermann, Handbook of Pulp and Papermaking, Second Edition, Elsevier, 1996.

[28] O. Faruk and M. Sain, Biofiber Reinforcement in Composite Materials, Kidlington: Woodhead, 2015.

[29] H. Tran and E. Vakkilainnen, "The Kraft Chemical Recovery Process," Tappi, 2008. [Online]. Available: http://www.tappi.org/content/events/08kros/manuscripts/1-1.pdf. [Accessed 11 March 2016].

[30] A. Pearson, "A Unified Theory of Refining," in *Pulp and Paper Technology Series*, 1990, p. 128.

[31] H. Yang, R. Yan, H. Chen, D. H. Lee and C. Zheng, "Characteristics of Hemicellulose, Cellulose, and Lignin Pyrolysis," *Fuel,* pp. 1781-1788, 2006.

[32] R. Reixach, J. Puig, J. A. Mendex, J. Girones, F. X. Espinach, G. Arbat and P. Mutje, "Orange Wood Fiber Reinforced Polypropylene Composites: Thermal Properties," *BioResources,* pp. 2156-2166, 2015.

[33] R. M. Rowell, A. R. Sanadi, D. F. Caulfield and R. E. Jacobson, "Utilization of Natural Fibers in Plastic Composites: Problems and Opportunities," *Lignocellulosic-Plastics Composites,* p. 1997, 23-51.

[34] X. Xu, "Cellulose Fiber Reinforced Nylon 6 or Nylon 66 Composites," *Georgia Institute of Technology,* p. Thesis, 2008.

[35] D. N. Saheb and J. Jog, "Natural Fiber Polymer Composites: A Review," *Advances in Polymer Technology,* vol. 18, no. 4, pp. 351-363, 1999.

[36] D. R. L. Vedoy, "Development of Methodologes for Improving Thermal Stability of Plant Fibers for Application in Thermoplastic Composites," *University of Waterloo,* p. Thesis, 2012.

[37] H.-S. Yang, M. P. Wolcott, H.-S. Kim, S. Kim and H.-J. Kim, "Effect of different compatibilizing agents on the mechanical properties of lignocellulosic material filled polyethylene bio-composites," *Composite Structures,* vol. 79, no. 3, pp. 369-375, 2006.

[38] L. Liu, B.-M. Zhang, D.-F. Wang and Z.-J. Wu, "Effects of cure cycles on void content and mechanical properties of composite laminates," *Compostive Structures,* vol. 79, no. 3, pp. 303-309, 2006.

[39] C. Dong and I. J. Davis, "Flexural Properties of Wheat Straw Reinforced Polyester Composites," *American Journal of Material Science,* vol. 1, no. 2, pp. 71-75, 2011.

[40] C. Klason, J. Kubát and H. Strömvall, "The Efficiency of Cellulosic Fillers in Common Thermoplastics. Part 1. Filling without Processing Aids or Coupling Agents," *International Journal of Polymeric Materials and Polymeric Biomaterials ,* vol. 10, no. 3, pp. 159-187, 1984.

[41] K. d. Sears and R. Jacobson, "Reinforcement of Engineering Thermoplastics with High Purity Wood Cellulose Fibers," *International Conference on Woodfiber-Plastic Composites,* pp. 27-34, 2001.

[42] E. Ozen, A. Kiziltas, E. E. Kiziltas and D. J. Gardner, "Natural Fiber Blend—Nylon 6 Composites," *Polymer Composites,* pp. 544-553, 2013.

[43] A. Kiziltas, D. J. Gardner, Y. Han and H.-S. Yang, "Mechanical Properties of Microcrystalline Cellulose (MCC) Filled Engineering Thermoplastic Composites," *Journal of Polymers and the Environment,* vol. 22, no. 3, pp. 365-372, 2014.

[44] A. Kiziltas, D. J. Gardner, Y. Han and H.-S. Yang, "Dynamic Mechanical behavior and thermal properties of microcrystalline cellulose (MCC)-filled nylon 6 composites," *Thermochimica Acta,* vol. 519, pp. 38-43, 2011.

[45] M. Misra, A. Mohanty, P. Tummala and L. Drzal, "Injection molded biocomposites from natural fibers and modified polyamide," in *ANTEC*, Chicago, 2004.

[46] K. D. Sears, R. E. Jacobson, D. F. Caulfield and J. Underwood, "Composites containing cellulosic pulp fibers and methods of making and using the same," *US6270883 B1,* 9 Oct 1998.

[47] U. Muller, M. Ratzsch, M. Schwanninger, M. Steiner and H. Zobl, "Yellowing and IR schanges of spruce wood as result of UV-irradiation," *Journal of Photochemistry and Photobiology,* vol. 69, no. 2, pp. 97-105, 2003.

[48] M. Deka, M. Humar, G. Rep, B. Kricej, M. Sentjurc and M. Petric, "Effects of UV light irradiation on colour stability of thermally modified, copper ethanolamine treated and non-modified wood: EPR and DRIFT spectroscopic studies," *Wood Science Technology,* vol. 42, no. 1, pp. 5-20, 2008.

[49] E. Fitzer and M. Heine, Fibre Reinforcements for Composite Materials, New York: Elsevier Science Publishers, 1988.

[50] A. Schiavo, "Carbon Fiber 2.0: Roadmap for Growth to 2020 and Beyond," in *Automotive Composites Conference and Exhibition*, Novi, 2015.

[51] N. G. Karsli and A. Aytac, "Tensile and thermomechanical properties of short carbon fiber reinforced polyamide 6 composites," *Composites Part B: Engineering,* vol. 51, pp. 270-275, 2013.

[52] S. Fua, B. Laukeb, E. Mäderb, C. Yuea and X. Hua, "Tensile properties of short-glass-fiber- and short-carbon-fiber-reinforced polypropylene composites," *Composites Part A: Applied Science and Manufacturing,* vol. 31, no. 10, pp. 1117-1125, 2000.

[53] Y. Kong and J. Hay, "The enthalpy of fusion and degree of crystallinity of polymers as measured by DSC," *European Polymer Journal,* vol. 39, no. 8, p. 1721–1727, 2003.

[54] TA Instruments, "Thermal Applications Note: Polymer Heats of Fusion," [Online]. Available: http://www.tainstruments.co.jp/application/pdf/Thermal_Library/Applications_Notes/TN048.PDF. [Accessed 30 March 2016].

[55] ASTM International, "Standard Test Method for Decomposition Kinetics by Thermogravimetry Using the Ozawa/Flynn/Wall Method," ASTM International, West Conshohocken, 2013.

[56] F. Yao, Q. Wu, Y. Lei, W. Guo and Y. Xu, "Thermal decomposition kinetics of natural fibers: Activation," *Polymer Degradation and Stability,* vol. 93, pp. 90-98, 2008.

[57] N. Zeng, S. L. Bai, C. G'Sell, J.-M. Hiver and Y. Mai, "Study on the microstructures and mechanical behaviour of compatibilized polypropylene/polyamide-6 blends," *Polymer International,* vol. 51, pp. 1439-1447, 2002.

[58] S.-L. Bai, G.-T. Wang, J.-M. Hiver and C. G'Sel, "Microstructures and mechanical properties of polypropylene/polyamide6/polyethelene-octene elastomer blends," *Polymer,* vol. 45, pp. 3063-3071, 2004.

[59] E. McHenry and Z. Stachurski, "Composite materials based on wood and nylon fibre," *Composites Part A; Applied Science and Manufacturing ,* vol. 34, no. 2, pp. 171-181, 2003.

[60] M. Garcia-Ramirez, J. Cavaillé, D. Dupeyre and A. Péguy, "Cellulose-polyamide 66 blends. I. Processing and characterization," *Journal of Polymer Science Part B: Polymer Physics,* vol. 32, no. 8, pp. 1437-1448, 1994.

[61] H. Ku, H. Wang, N. Pattarachaiyakoop and M. Trada, "A review on the tensile properties of natural fiber reinforced polymer composites," *Composites: Part B,* vol. 42, pp. 856-873, 2011.

[62] A. Kiziltas, D. J. Gardner, Y. Han and H.-S. Yang, "Determining the Mechanical Properties of Microcrystalline Cellulose (MCC)-Filled PET-PTT Blend Composites," *Wood and Fiber Science,* vol. 42, no. 2, pp. 165-176, 2010.

[63] A. Rudin, The Elements of Polymer Science and Engineering, 2nd Edition ed., San Diego, CA: Academic Press, 1999, p. 380.

[64] A. Kiziltas, D. J. H. Y. Gardner and H.-S. Yang, "Thermal properties of microcrystalline cellulose-filled PET-PTT blend polymer composites," *Journal of Thermal Analysis and Calorimetry,* vol. 103, pp. 163-170, 2010.

[65] Y. Feng, X. Jin and J. Hay, "Effect of nucleating agent addition on crystallization of isotactic polypropylene," *Journal of Applied Polymer Science,* vol. 69, no. 10, p. 2089–2095, 1998.

[66] R. Dweiri and C. Azhari, "Thermal and Flow Property–Morphology Relationship ofSugarcane Bagasse Fiber-Filled Polyamide 6 Blends," *Journal of Applied Polymer Science,* vol. 92, pp. 3744-3754, 2004.

[67] P. C. Painter, S. L. Shenoy, D. E. Bhagwagar, J. Fishburn and M. M. Coleman, "Effect of Hydrogen Bonding on the Melting Point Depression in Polymer Blends Where One Component Crystallizes," *Macromolecules,* vol. 24, no. 20, pp. 5623-5629, 1991.

[68] M. Garcia-Ramirez, J. Cavaille, D. Dupeyre and A. Peguy, "Cellulose-Polyamide 66 Blends. Processing and Characterization," *Journal of Polymer Science Part B: Polymer Physics,* vol. 32, no. 8, pp. 1437-1448, 1994.

[69] H. Seefeldt, "Fire retardancy of wood-plastic composites," *Thesis submitted to The Technical University of Berlin,* 2012.

[70] RTP Company, "NYLON 6/12 (PA)," 2014. [Online]. Available: http://www.rtpcompany.com/products/product-guide/nylon-612-pa-polyamide-612/. [Accessed 20 November 2014].

[71] E. Bolton, "Development of Nylon," *Industrial and Engineering Chemistry,* vol. 35, no. 1, pp. 53-58, January 1942.

[72] H. Hager and J. Limper, "High-Tech Plastics from the Field," *Evonik Science Newsletter,* pp. 24-30.

[73] L. Shen, J. Haufe and M. K. Patel, "Product overview and market projection of emerging bio-based plastics," Group Science, Technology and Society, Netherlands, 2009.

[74] L. Trossarelli, "The History of Nylon," Turin University, 9 March 2002. [Online]. [Accessed 20 November 2014].

[75] R. P. Wool and X. S. Sun, Bio-Based Polymers and Composites, Elsevier Academic Press, 2005.

[76] E. o. D. i. C. Materials, Wilkins, Dick J., Philadelphia: ASTM Special Technical Publications, 1984.

Appendix A – Material Specifications

PA610

Important properties of VESTAMID® *Terra* HS

Property	Test method	Unit	HS16	HS18	HS22	HS18–GF30
Viscosity number	ISO 307	cm³/g	160	180	220	180
Melting temperature	ISO 11357	°C	223	223	223	223
Glass transition temp.		°C	48	48	48	48
Water absorption at RT	Evonik	%	3.3	3.3	3.3	2.3
Density	ISO 1183	g/cm³	1.06	1.07	1.08	1.32
VICAT softening temp.	ISO 306					
Method B 50 N		°C	196	196	196	217
Tensile test	ISO 527					
Stress at yield		MPa	61	61	61	147
Strain at yield		%	5	5	5	4
Strain at break		%	>50	> 50	> 50	4
Tensile modulus	ISO 527	MPa	2100	2100	2100	8300
CHARPY 23 °C	ISO 179/1eU	kJ/m²	N	N	N	89 C
impact strength −30 °C		kJ/m²	N	N	N	88 C
CHARPY notched 23 °C	ISO 179/1eA	kJ/m²	6 C	7 C	7 C	16 C
impact strength −30 °C		kJ/m²	6 C	6 C	6 C	10 C
Biobased content	ASTM 6866	% of C	63	63	63	44
Global warming potential[1]	ISO 14040	kg CO_{2eq}	4.6	4.6	4.6	5.1

N = no break   C = complete break   1) Reference year: 2010, Evaluation method: CML2001

PA1010

Important properties of VESTAMID® *Terra* DS

Property	Test method	Unit	DS16	DS18	DS22	DS18–GF30
Viscosity number	ISO 307	cm³/g	160	180	220	180
Melting temperature	ISO 11357	℃	200	200	200	200
Glass transition temp.		℃	37	37	37	37
Water absorption at RT	Evonik	%	1.8	1.8	1.8	1.4
Density	ISO 1183	g/cm³	1.05	1.06	1.07	1.29
VICAT softening temp.	ISO 306					
Method B 50 N		℃	171	171	171	196
Tensile test	ISO 527					
Stress at yield		MPa	54	54	54	136
Strain at yield		%	5	5	5	4
Strain at break		%	>50	> 50	> 50	5
Tensile modulus	ISO 527	MPa	1700	1700	1700	7400
CHARPY 23 ℃	ISO 179/1eU	kJ/m²	N	N	N	95 C
impact strength −30 ℃		kJ/m²	N	N	N	96 C
CHARPY notched 23 ℃	ISO 179/1eA	kJ/m²	7 C	7 C	11 C	19 C
impact strength −30 ℃		kJ/m²	7 C	7 C	14 C	11 C
Biobased content	ASTM 6866	% of C	100	100	100	70
Global warming potential[1]	ISO 14040	kg CO_{2eq}	4.0	4.0	4.0	4.6

N = no break   C = complete break   1) Reference year: 2010, Evaluation method: CML2001

Recycled PA 6

Engineering Grade Nylon 6 Resin

Property	ISO Test Method	Metric Units		Standard Units	
Tensile Strength	527-93	MPa	75	psi*	10,900
Tensile Elongation	527-93	%	60	%	60
Flexural Modulus	178-93	MPa	2,700	psi*(10^5)	3.9
Flexural Strength	178-93	MPa	95	psi*	13,800
Izod Impact	180-93	kJ/m^2	6	ft-lbs/in*	1.1
HDT @ 264 psi	75-93	°C	55	°F	130
Density	1183-87	g/cc	1.14	g/cc	1.14
Melting Point	3146	°C	220	°F	430
Shrinkage - Flow	DIS 294-4	%	1.1 – 1.5	%	1.1 – 1.5
Shrinkage - Transverse	DIS 294-4	%	1.2 – 1.6	%	1.2 – 1.6
Filler Content	3451-4	%	0	%	0

Cellulose

CreaTech TC 200 Product Data	
Typical Physical Properties	
Appearance	White Fiber
Alpha cellulose content	99.5% minimum, dry base
Loose Density	>40 grams/liter
Moisture Content	<7.5%
pH Value	5-7.5
Ash Content	0.4% maximum
Brightness	>86
Average Percent of Retained Fiber - 200 micron (US 70)	<2%
Heavy Metals	<10 ppm
Average Fiber Size	Length: 155 micron Width: 20 micron Thickness: 1-2 micron
Standard Packaging	
Bag Type	6 mil polyethylene
Bag weight (net)	20 kg

Bags per pallet	36 bags
Pallet	45x45 in.
Certifications and Standards	
CreaFill Fibers is ISO 9001:2008 Certified	
Supplied by CreaFill Fibers Corp.	

Carbon Fiber

Milled fiber without sizing

Brand name	Production site	Type	Cut length	Sizing	Size level	Bulk density
Tenax®-A		HT M100	60 µm 100 µm	---	---	550 g/l 400 g/l

Appearance

Form	Solid, short fibers
Color	Black
Odor	Odorless

Basic physical and chemical properties

Inflammability and explosion limits

Upper	Not applicable
Lower	Not applicable
Oxidizing properties	None
Density 23 °C [g/cm³]	1.7 - 2.0
Bulk weight [g/l]	250 - 650
Melting point [°C]	ca. 3500
Decomposition temp.	≥ 650 (ambient air), Sizing ≥ 290

Other information

Spec. electr. contuctivity	1.6×10^{-3} Ohm cm

TECHNICAL DATA

STRUKTOL® RP 17

ODOR NEUTRALIZING/MASKING PROCESS ADDITIVE

COMPOSITION

Proprietary blend.

PROPERTIES	TYPICAL VALUES
Appearance	White pastille
Dropping point (°C)	108 - 115
Specific Gravity	0.94
Storage Stability	At least 2 years under normal storage conditions
Packaging	55 lb. bag

RECOMMENDATIONS FOR APPLICATION

STRUKTOL® RP 17 may be added during compounding, extrusion or molding to eliminate or mask undesirable odors often associated with the addition of post-industrial or post-consumer recyclate streams or other ingredients used in compounding. This product was developed as an odor mask for PE and PP WPC products where, in some cases, the fillers or the recycled plastic in a formula imparted unpleasant odors in the final product. The product is particularly applicable for automotive applications where higher process temperatures may make the odors more noticeable. At low dosages it tends to neutralize odor while at higher dosages it will impart a fresh "clean" odor. Although developed for WPC products, it has been shown to work well in plain recycled PE and PP products, as well as various rubber products.

STRUKTOL® RP 17 is not FDA. If FDA is needed, please refer to STRUKTOL® SA 1259 in a powder form and STRUKTOL® SA 1346 in a pastille form.

DOSAGE

Plastics: A starting use level would be 0.5%, however more or less may be required to obtain desired odor elimination.

Rubber: 2 – 5%

(5/7/2014)JMB/MSF/SNK/rca

Appendix B – ANOVA Tables

Table 10: Anova Table for 20% Suzano Fiber vs 20% WF2 Fiber

	DF	SS	MS	F	$F_{crit}(\alpha = 0.05)$	Conclusion
Polyamide	2	4263010	2131505	260.75	3.28	Significant
Fiber	1	9637	9636.71	1.18	4.13	Insignificant
Interaction	2	534462	304398.3	37.24	3.28	Significant
Error	34	277932	8174.5			
Total	39	5085041				

Table 11: Anova Table for 30% Suzano Fiber vs 30% WF2 Fiber

	DF	SS	MS	F	$F_{crit}(\alpha = 0.05)$	Conclusion
Polyamide	2	4123791	2061895	142.36	3.28	Significant
Fiber	1	201873	201873	13.94	4.13	Significant
Interaction	2	25674	12837	0.89	3.28	Insignificant
Error	38	550380	14484			
Total	43	4901717				

Table 12: Anova Table for 20% Suzano Fiber vs 30% Suzano Fiber

	DF	SS	MS	F	$F_{crit}(\alpha = 0.05)$	Conclusion
Polyamide	2	5394348	2697174	213.36	3.28	Significant
Fiber	1	476021	476021	37.66	4.13	Significant
Interaction	2	603386	301693	23.87	3.28	Significant
Error	42	530943	12641			
Total	47	7004698				

Table 13: Anova Table for 20% WF2 Fiber vs 30% WF2 Fiber

	DF	SS	MS	F	$F_{crit}(\alpha = 0.05)$	Conclusion
Polyamide	2	2001617	1000809	105.49	3.28	Significant
Fiber	1	1266032	1266032	133.44	4.13	Significant
Interaction	2	471633	235816	24.86	3.28	Significant
Error	34	322571	9487			
Total	39	4061853				

Table 14: ANOVA Table for RP17 content vs Flex Modulus

	DF	SS	MS	F	$F_{crit}(\alpha = 0.05)$	Conclusion
Factor	1	0.0129	0.0129	7.99	5.32	Significant
Error	8	0.0129	0.00162			
Total	9	0.0258				

Table 15: ANOVA Table for RP17 content vs Stress at 5% Strain

	DF	SS	MS	F	$F_{crit}(\alpha = 0.05)$	Conclusion
Factor	1	3.08	3.08	1.53	5.32	Insignificant
Error	8	16.1	2.02			
Total	9	19.2				

Table 16: ANOVA Table for RP17 content vs Young's Modulus

	DF	SS	MS	F	$F_{crit}(\alpha = 0.05)$	Conclusion
Factor	1	756584	756584	34.4	4.96	Significant
Error	10	219901	21990			
Total	11	976485				

Table 17: ANOVA Table for RP17 content vs Tensile Stress at Maximum Load

	DF	SS	MS	F	$F_{crit}(\alpha = 0.05)$	Conclusion
Factor	1	91.6	91.6	56.6	4.96	Significant
Error	10	16.2	1.62			
Total	11	108				

Table 18: ANOVA Table for RP17 content vs Impact Strength

	DF	SS	MS	F	$F_{crit}(\alpha = 0.05)$	Conclusion
Factor	1	982	982	15.7	4.49	Significant
Error	16	1000	62.5			
Total	17	1982				

Appendix C – Equation Derivations

Equation 2: $X_{C_{PP}} = \dfrac{\Delta\widehat{H}_{f_{PP}}}{m_{PP}\Delta\widehat{H}^{\circ}_{f_{PP}}}$

Given Equation 1:

$$X_c = \frac{\Delta H_f}{\Delta H^{\circ}_f}$$

And Data Available is $\Delta\widehat{H}_{f_i}$ and $\Delta\widehat{H}^{\circ}_{f_i}$ $\left[\dfrac{J}{g}\right]$

$$\Delta H_f = \Delta\widehat{H}_f \times mass\ of\ sample\ (M_{total})$$

$$\Delta H^{\circ}_f = \Delta\widehat{H}^{\circ}_f \times mass\ of\ polymer\ present\ to\ crystallize\ (M_i)$$

Therefore, equation 1 can be replaced with:

$$X_{C_i} = \frac{\Delta\widehat{H}_f \times M_{total}}{\Delta\widehat{H}^{\circ}_f \times M_i} = \frac{\Delta\widehat{H}_f}{\Delta\widehat{H}^{\circ}_f \times \left(\frac{M_i}{M_{total}}\right)} = \frac{\Delta\widehat{H}_{f_i}}{\Delta\widehat{H}^{\circ}_{f_i} \times m_i}$$

Where m_i is the mass fraction of the crystallisable phase.

Equation 3: $X_{C_{PA}} = \dfrac{\Delta\widehat{H}_{f_{PA}}}{m_{PA610}\Delta\widehat{H}^{\circ}_{f_{PA610}}+m_{PA6}\Delta\widehat{H}^{\circ}_{f_{PA6}}}$

Starting from Equation 2:

$$X_{C_i} = \frac{\Delta\widehat{H}_{f_i}}{\Delta\widehat{H}^{\circ}_{f_i} \times m_i}$$

The reference for 100% crystalline enthalpy of fusion is approximated by a linear combination of the two individual polyamide references, referred to here as A and B.

$$\Delta\widehat{H}^{\circ}_{f_i} = \frac{m_A}{m_A + m_B}\Delta\widehat{H}^{\circ}_{f_A} + \frac{m_B}{m_A + m_B}\Delta\widehat{H}^{\circ}_{f_B}$$

The mass fraction used in Equation 2 is the summation of the two polyamide mass fractions

$$m_i = m_A + m_B$$

Subbing these two adjustments into Equation 2:

$$X_{c_{PA}} = \frac{\Delta \widehat{H}_{f_{PA}}}{(m_A + m_B) \times \left(\frac{m_A}{m_A + m_B} \Delta \widehat{H}^{\circ}_{f_A} + \frac{m_B}{m_A + m_B} \Delta \widehat{H}^{\circ}_{f_B} \right)}$$

This simplifies to:

$$X_{c_{PA}} = \frac{\Delta \widehat{H}_{f_{PA}}}{m_A \Delta \widehat{H}^{\circ}_{f_A} + m_B \Delta \widehat{H}^{\circ}_{f_B}}$$

Appendix D – Additional Experimental Data

TGA Curves of Natural Fibers, separated by Fiber Type

Suzano Air
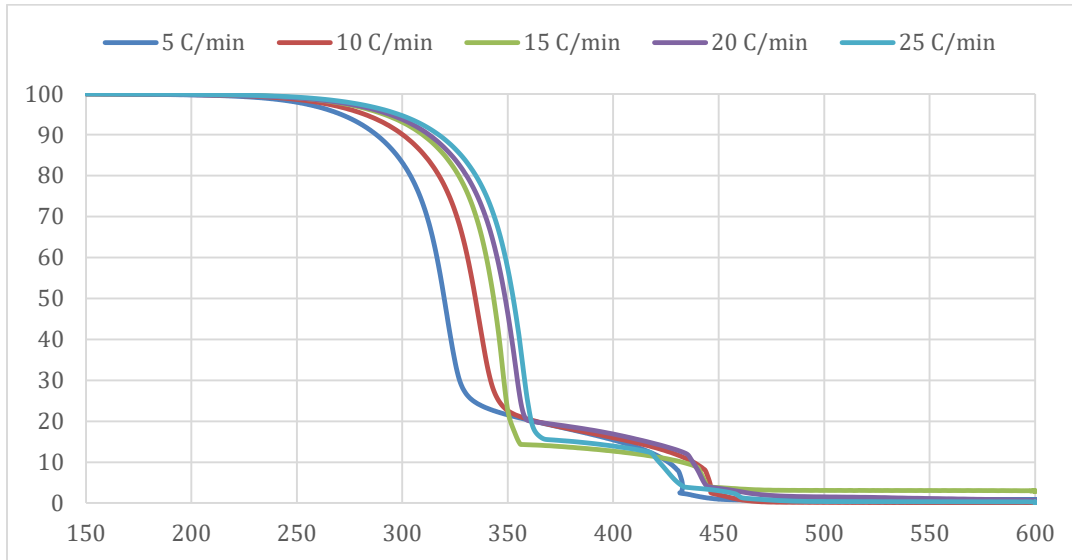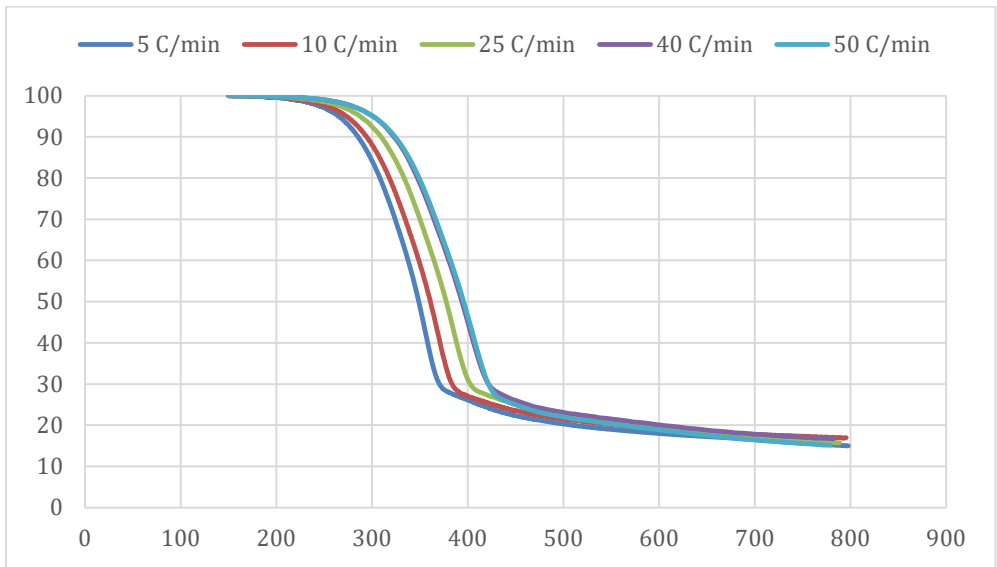

Suzano Nitrogen
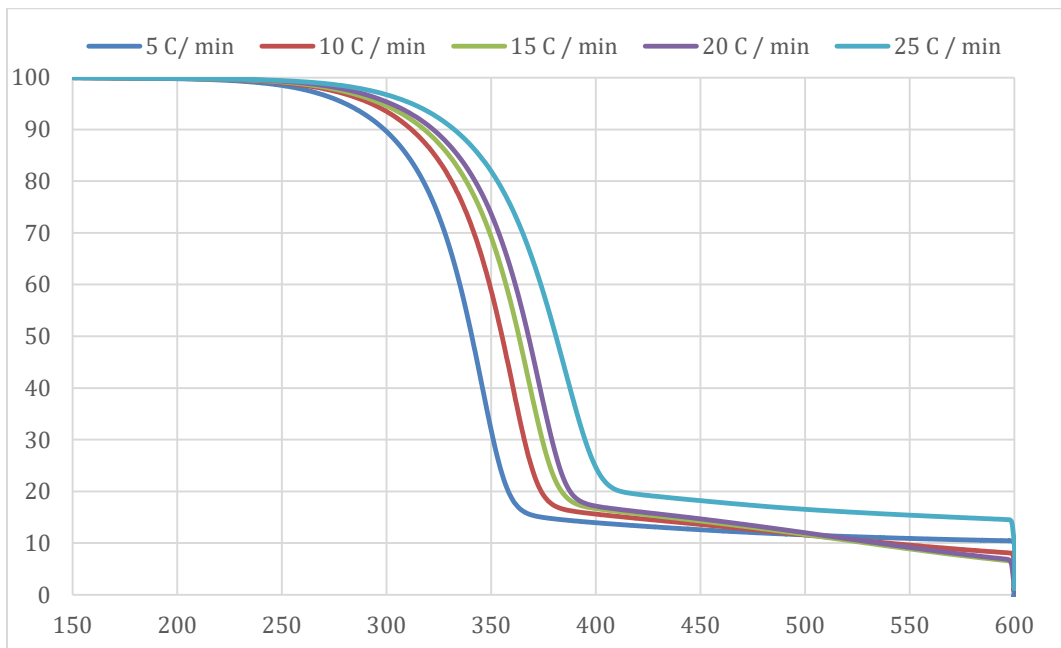
Woodforce 1 Air
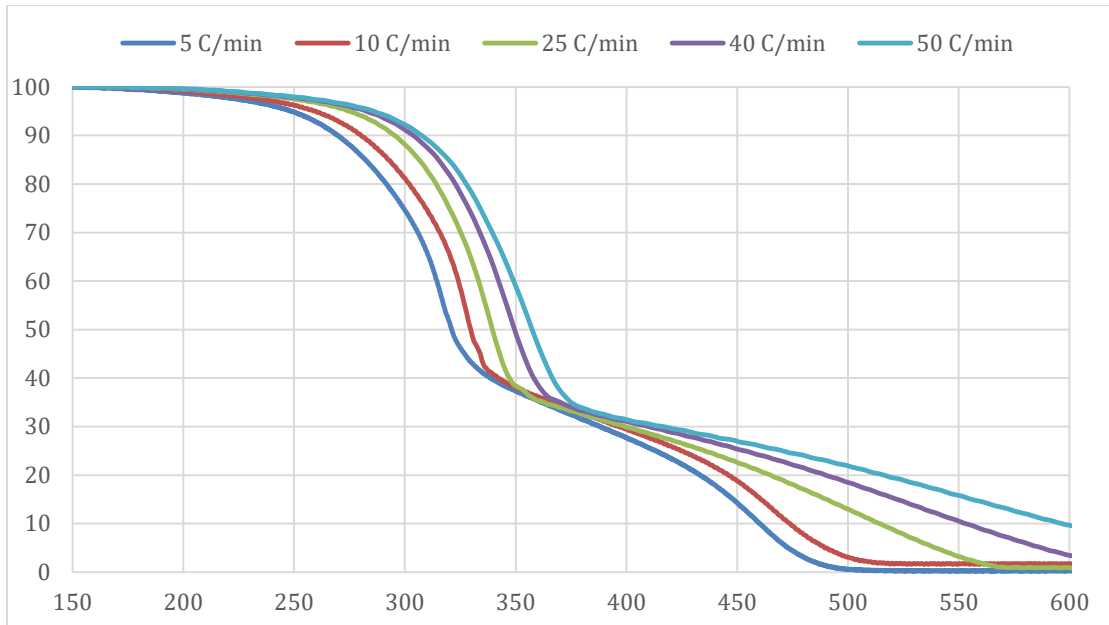
Woodforce 1 Nitrogen
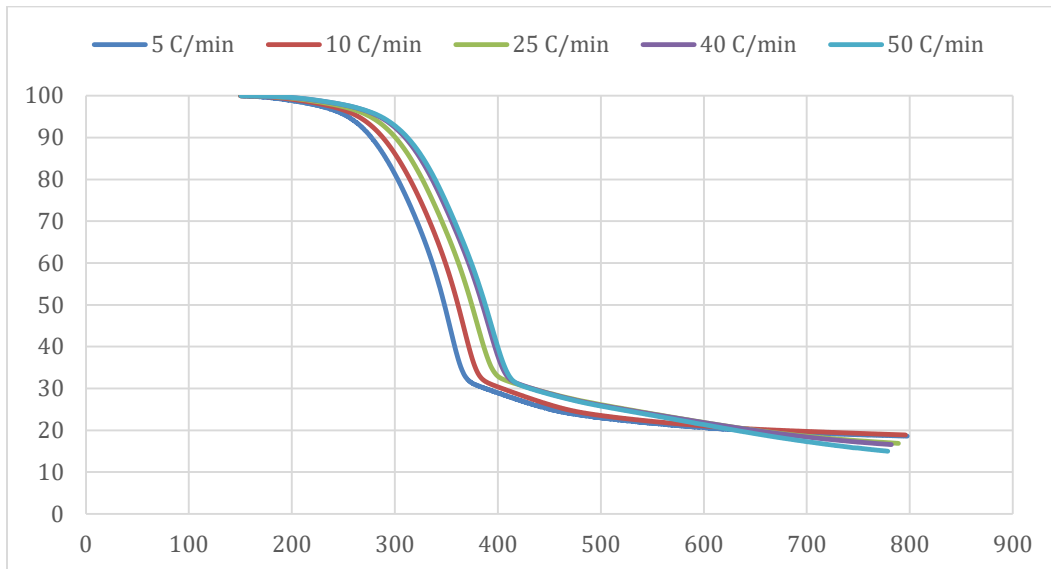
Woodforce 2 Air
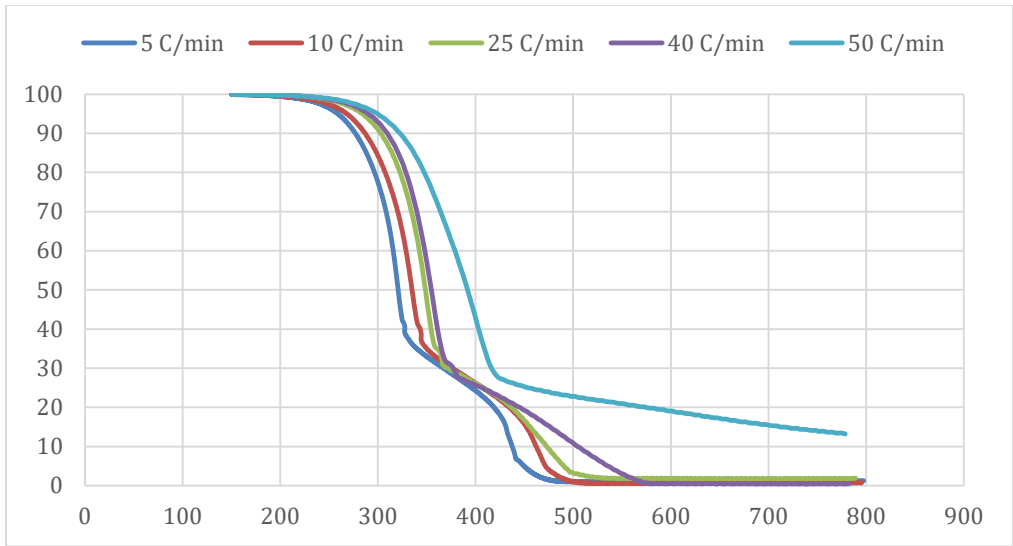
Woodforce 2 Nitrogen

SEM Image Analysis

Figure 48, below, shows the particle analysis results of the Image J software.
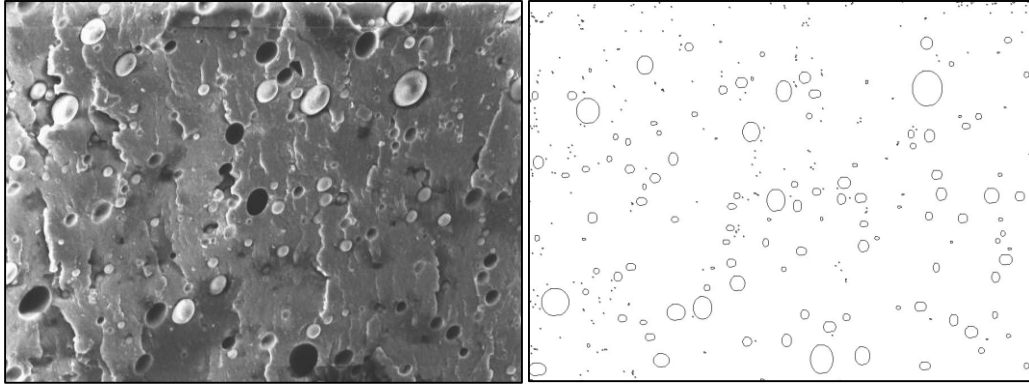

Figure 48 – Image J Ellipse Fit Results

The pixel area of each fitted circle was added and compared to the total number of pixels of the image. This ratio of 6.1% was then approximated to be the volume fraction of polypropylene in the composite. Figure 49 shows a histogram of the approximate sizes of each fitted particle.
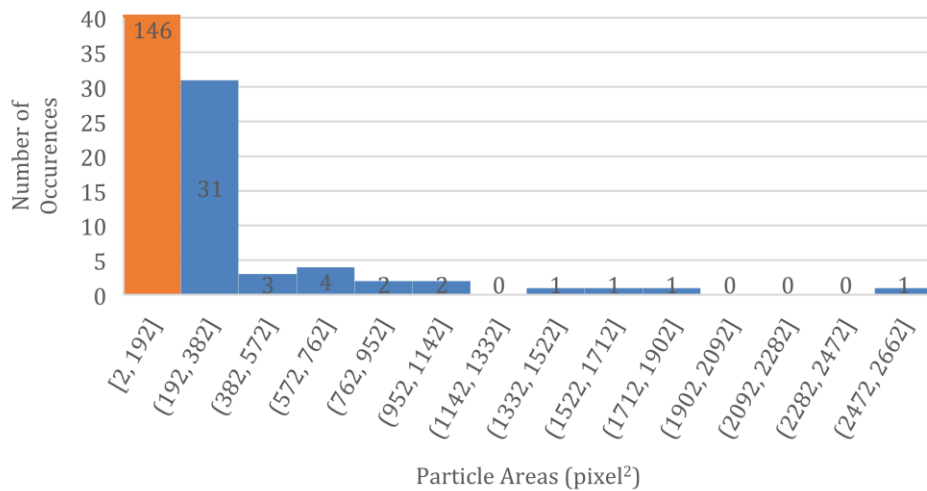

Figure 49 – Image J Particle Analysis Histogram